Weak pion production off the nucleon

E. Hernández,[1] J. Nieves,[2] and M. Valverde[2]

[1]*Grupo de Física Nuclear, Departamento de Física Fundamental e IUFFyM, Universidad de Salamanca, E-37008 Salamanca, Spain.*
[2]*Departamento de Física Atómica, Molecular y Nuclear, Universidad de Granada, E-18071 Granada, Spain*

(Received 18 January 2007; published 23 August 2007)

We develop a model for the weak pion production off the nucleon, which besides the delta pole mechanism [weak excitation of the $\Delta(1232)$ resonance and its subsequent decay into $N\pi$], includes also some background terms required by chiral symmetry. We refit the $C_5^A(q^2)$ form factor to the flux-averaged $\nu_\mu p \to \mu^- p \pi^+$ ANL q^2-differential cross section data, finding a substantially smaller contribution of the delta pole mechanism than traditionally assumed in the literature. Within this scheme, we calculate several differential and integrated cross sections, including pion angular distributions, induced by neutrinos and antineutrinos and driven both by charged and neutral currents. In all cases we find that the background terms produce quite significant effects, and that they lead to an overall improved description of the data, as compared to the case where only the delta pole mechanism is considered. We also show that the interference between the delta pole and the background terms produces parity-violating contributions to the pion angular differential cross section, which are intimately linked to T-odd correlations in the contraction between the leptonic and hadronic tensors. However, these latter correlations do not imply a genuine violation of time-reversal invariance because of the existence of strong final state interaction effects.

DOI: 10.1103/PhysRevD.76.033005 PACS numbers: 25.30.Pt, 12.15.−y, 12.39.Fe, 13.15.+g

I. INTRODUCTION

The pion production processes from nucleons and nuclei at intermediate energies are important tools to study the hadronic structure and have become very important in the analysis of the neutrino oscillation experiments with atmospheric neutrinos. The energy spectrum of atmospheric neutrinos at Kamioka [1] is such that the weak pion production contributes about 20% of the quasielastic lepton production, and it is a major source of uncertainty in the identification of electron and muon events. In particular, the neutral current (NC) π^0 production contributes to the background of $e^\pm$ production while $\pi^\pm$ contributes to the background of $\mu^\pm$ production. This is because both particles, i.e., π^0 and $e^\pm$ or $\pi^\pm$ and $\mu^\pm$, produce similar single-ring events in Cherenkov detectors, commonly used in neutrino oscillation experiments. Moreover, the neutral current π^0 production might play an important role in distinguishing between the two oscillation mechanisms $\nu_\mu \to \nu_\tau$ and $\nu_\mu \to \nu_{\text{sterile}}$ [2]. These comments apply also for ν_e appearance experiments such as K2K [3] and MiniBooNE [4].

The neutrino oscillation experiments are generally performed with detectors which use material with nuclei like ^{12}C, ^{16}O, etc., as targets. It is therefore desirable that nuclear medium effects be studied in the production of leptons and pions induced by the atmospheric as well as accelerator neutrinos used in these oscillation experiments. To this end, the starting point should be a correct understanding of the reaction mechanisms in the free space. In this context we study in this work the weak pion production off the nucleon driven both by charged currents (CC) and NC at intermediate energies. The model derived here will allow us to extend the results of Refs. [5,6] for CC and Ref. [7] for NC driven neutrino-nucleus reactions in the quasielastic region to higher excitation energies above the pion production threshold up to the $\Delta(1232)$ peak.

In the past, there have been several studies of the weak pion production off the nucleon at intermediate energies [8–19]. Most of them describe the pion production process at intermediate energies[1] by means of the delta pole (ΔP) mechanism [weak excitation of the $\Delta(1232)$ resonance and its subsequent decay into $N\pi$] and do not incorporate any background terms. Here, we have also included some background terms, required by chiral symmetry. Starting from an SU(2) nonlinear σ model involving pions and nucleons, which implements the pattern of spontaneous chiral symmetry breaking of QCD, we derive the corresponding vector and axial currents [up to order $\mathcal{O}(1/f_\pi^3)$] which determine the structure of the chiral nonresonant terms. Some background terms were also considered in Refs. [11,12,15]. In the third reference, the chiral counting was broken to account explicitly for ρ and ω exchanges in the t-channel, while the first two works are not consistent with the chiral counting either, since contact terms were not included. Moreover in [11,12] a rather small axial mass (≈ 0.65 GeV) was used.

We will show that the background terms produce quite significant effects, which will require readjusting the $C_5^A(q^2)$ form factor that controls the largest term of the Δ-axial contribution. We will find corrections of the order of 30% to the off-diagonal Goldberger-Treiman relation

[1]Higher resonance effects, which are certainly important for energies larger than those considered in this work, are carefully discussed in Ref. [19].

when the Argonne bubble chamber cross section data [20] are fitted. Such corrections would be smaller if the Brookhaven bubble chamber data [21] were considered. We will also show that interference between the ΔP and the background terms produces parity-violating contributions to the pion angular differential cross section, which are intimately linked to T-odd correlations in the contraction between the leptonic and hadronic tensors. However, these T-odd correlations do not imply a genuine violation of time-reversal invariance because of the existence of strong final state interaction effects.

The paper is organized as follows. After this introduction, in Sec. II the model for CC neutrino- and antineutrino-induced reactions is presented. There, some general definitions involving kinematics and differential cross sections are given (Sec. II A). The consequences of isospin symmetry are exploited in Sec. II B, while in the next subsection the model for the $WN \to N'\pi$ reaction is presented. In Sec. III, the findings of the latter section are extended to the case of NC driven processes. Results are presented and discussed in Sec. IV and the main conclusions of this work can be found in Sec. V. In Appendix A, the cross section dependence on the pion azimuthal angle is discussed in terms of Lorentz, parity, and time-reversal invariances, and finally in Appendix B, we discuss in some detail the effects on the neutrino- and antineutrino-induced cross sections of different relative signs between the axial and vector $W^{\pm}\Delta N$ form factors, and between the resonant and chiral nonresonant contributions.

II. CC NEUTRINO- AND ANTINEUTRINO-INDUCED REACTIONS

A. Kinematics and differential cross section

We will focus on the neutrino-pion production reaction off the nucleon driven by charged currents,

$$\nu_l(k) + N(p) \to l^-(k') + N(p') + \pi(k_\pi), \qquad (1)$$

though the generalization of the obtained expressions to antineutrino-induced reactions is straightforward.

The unpolarized differential cross section, with respect to the outgoing lepton and pion kinematical variables, is given in the laboratory (LAB) frame (the kinematics is sketched in Fig. 1) by[2]

$$\frac{d^5\sigma_{\nu_l l}}{d\Omega(\hat{k}')dE'd\Omega(\hat{k}_\pi)} = \frac{|\vec{k}'|}{|\vec{k}|}\frac{G^2}{4\pi^2}\int_0^{+\infty}\frac{d|\vec{k}_\pi||\vec{k}_\pi|^2}{E_\pi} \times L^{(\nu)}_{\mu\sigma}(W^{\mu\sigma}_{CC\pi})^{(\nu)}, \qquad (2)$$

[2]To obtain Eq. (2) we have neglected the four-momentum carried out by the intermediate W-boson with respect to its mass (M_W), and have used the existing relation between the gauge weak coupling constant, $g = e/\sin\theta_W$ and the Fermi constant: $G/\sqrt{2} = g^2/8M_W^2$, with e the electron charge, θ_W the Weinberg angle, and M_W the W-boson mass.

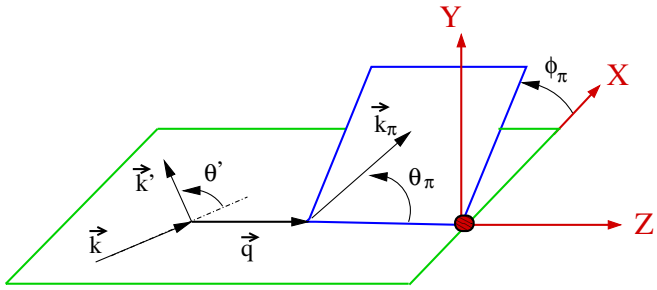

FIG. 1 (color online). Definition of the different kinematical variables used through this work.

with $\vec{k}$ and $\vec{k}'$ the LAB lepton momenta, $E' = (\vec{k}'^2 + m_l^2)^{1/2}$ and m_l the energy and the mass of the outgoing lepton ($m_\mu = 105.65$ MeV, $m_e = 0.511$ MeV), $G = 1.1664 \times 10^{-11}$ MeV^{-2} the Fermi constant, $\vec{k}_\pi$ and $E_\pi = (\vec{k}_\pi^2 + m_\pi^2)^{1/2}$ the LAB momentum and energy of the outgoing pion,[3] and L and W the leptonic and hadronic tensors, respectively. The leptonic tensor is given by [in our convention, we take $\epsilon_{0123} = +1$ and the metric $g^{\mu\nu} = (+,-,-,-)$]

$$L^{(\nu)}_{\mu\sigma} = (L^{(\nu)}_s)_{\mu\sigma} + i(L^{(\nu)}_a)_{\mu\sigma} = k'_\mu k_\sigma + k'_\sigma k_\mu - g_{\mu\sigma}k\cdot k' + i\epsilon_{\mu\sigma\alpha\beta}k'^\alpha k^\beta, \qquad (3)$$

and it is not orthogonal to q^μ even for massless neutrinos, i.e, $L^{(\nu)}_{\mu\sigma}q^\mu = -m_l^2 k_\sigma$.

The hadronic tensor includes all sorts of nonleptonic vertices, and it reads

$$(W^{\mu\sigma}_{CC\pi})^{(\nu)} = \frac{1}{4M}\bar{\sum_{spins}}\int\frac{d^3p'}{(2\pi)^3}\frac{1}{2E'_N}\delta^4(p' + k_\pi - q - p) \times \langle N'\pi|j^\mu_{cc+}(0)|N\rangle\langle N'\pi|j^\sigma_{cc+}(0)|N\rangle^*, \qquad (4)$$

with M the nucleon mass,[4] $q = k - k'$, and E'_N the energy of the outgoing nucleon. The bar over the sum of initial and final spins denotes the average on the initial ones. As for the one particle states, they are normalized so that $\langle\vec{p}|\vec{p}'\rangle = (2\pi)^3 2p_0\delta^3(\vec{p} - \vec{p}')$, and finally for the charged current which couples to the W^+ we take

$$j^\mu_{cc+} = \bar{\Psi}_u\gamma^\mu(1 - \gamma_5)(\cos\theta_C\Psi_d + \sin\theta_C\Psi_s) \qquad (5)$$

with Ψ_u, Ψ_d, and Ψ_s quark fields, and θ_C the Cabibbo angle ($\cos\theta_C = 0.974$). Note that with all these definitions, the matrix element $\langle N'\pi|j^\mu_{cc}(0)|N\rangle$ is dimensionless. After performing the d^3p' integration, there will still be left an energy conserving Dirac's delta function $[\delta(p'^0 + k^0_\pi - q^0 - p^0)]$ in the hadronic tensor, which can be used to perform the $d|\vec{k}_\pi|$ integration in Eq. (2). Since the quantity $\int d\Omega_\pi L^{(\nu)}_{\mu\sigma}(W^{\mu\sigma}_{CC\pi})$ is a scalar, to evaluate it we take for

[3]For m_π, we use the isospin averaged pion mass.
[4]We take the average of the neutron and proton masses.

convenience $\vec{q}$ in the Z direction. Referring now the pion variables to the outgoing πN pair center of mass (CM) frame (as is usual in pion electroproduction) would be readily done by means of a boost in the Z direction. Note that the azimuthal angle ϕ_π is left unchanged by such a boost.

By construction, the hadronic tensor accomplishes

$$(W^{\mu\sigma}_{\mathrm{CC}\pi})^{(\nu)} = (W^{\mu\sigma}_{\mathrm{CC}\pi})^{(\nu)}_s + \mathrm{i}(W^{\mu\sigma}_{\mathrm{CC}\pi})^{(\nu)}_a, \tag{6}$$

with $(W^{\mu\sigma}_{\mathrm{CC}\pi})^{(\nu)}_s$ and $(W^{\mu\sigma}_{\mathrm{CC}\pi})^{(\nu)}_a$ the real symmetric and antisymmetric parts, respectively.

As is explicitly shown in Appendix A, Lorentz invariance restricts the ϕ_π dependence,

$$\frac{d^5\sigma_{\nu_l l}}{d\Omega(\hat{k}')dE'd\Omega(\hat{k}_\pi)} = \frac{|\vec{k}'|}{|\vec{k}|}\frac{G^2}{4\pi^2}\{A + B\cos\phi_\pi + C\cos 2\phi_\pi + D\sin\phi_\pi + E\sin 2\phi_\pi\}, \tag{7}$$

with A, B, C, D, and E real structure functions, which depend on q^2, $p\cdot q$, $k_\pi\cdot q$, and $k_\pi\cdot p$.

For antineutrino-induced reactions we have

$$L^{(\bar{\nu})}_{\mu\sigma} = L^{(\nu)}_{\sigma\mu}, \tag{8}$$

and we will discuss below the existing relation between the matrix elements of $j^\mu_{\mathrm{cc}+}$ and $j^\mu_{\mathrm{cc}-} = j^{\mu\dagger}_{\mathrm{cc}+}$, charged currents which couple to the W^+ and W^- bosons, respectively.

B. Isospin relations

The nonstrange parts of $j^\mu_{\mathrm{cc}\pm}$ behave as the spherical ± 1 component of an isovector, since

$$\bar{\Psi}_u\Psi_d = -\bar{\Psi}_q\frac{\tau^1_{+1}}{\sqrt{2}}\Psi_q, \qquad \bar{\Psi}_d\Psi_u = \bar{\Psi}_q\frac{\tau^1_{-1}}{\sqrt{2}}\Psi_q,$$
$$\Psi_q = \begin{pmatrix}\Psi_u\\ \Psi_d\end{pmatrix}, \qquad \tau^1_0 = \tau_z, \qquad \tau^1_{\pm 1} = \mp\frac{\tau_x \pm \mathrm{i}\tau_y}{\sqrt{2}}, \tag{9}$$

with $\vec{\tau}$ the Pauli matrices. Thanks to the Wigner-Eckart's theorem, we find that all $\langle N'\pi|j^\mu_{\mathrm{cc}\pm}(0)|N\rangle$ matrix elements are determined by just two of them, for instance, $\langle p\pi^+|j^\mu_{\mathrm{cc}+}(0)|p\rangle$ and $\langle n\pi^+|j^\mu_{\mathrm{cc}+}(0)|n\rangle$:

$$\langle p\pi^0|j^\mu_{\mathrm{cc}+}(0)|n\rangle = -\frac{1}{\sqrt{2}}[\langle p\pi^+|j^\mu_{\mathrm{cc}+}(0)|p\rangle - \langle n\pi^+|j^\mu_{\mathrm{cc}+}(0)|n\rangle], \tag{10}$$

$$\langle p\pi^-|j^\mu_{\mathrm{cc}-}(0)|p\rangle = \langle n\pi^+|j^\mu_{\mathrm{cc}+}(0)|n\rangle, \tag{11}$$

$$\langle n\pi^-|j^\mu_{\mathrm{cc}-}(0)|n\rangle = \langle p\pi^+|j^\mu_{\mathrm{cc}+}(0)|p\rangle, \tag{12}$$

$$\langle n\pi^0|j^\mu_{\mathrm{cc}-}(0)|p\rangle = -\langle p\pi^0|j^\mu_{\mathrm{cc}+}(0)|n\rangle = \frac{1}{\sqrt{2}}[\langle p\pi^+|j^\mu_{\mathrm{cc}+}(0)|p\rangle - \langle n\pi^+|j^\mu_{\mathrm{cc}+}(0)|n\rangle]. \tag{13}$$

Thus, Eqs. (8) and (11)–(13) allow us to determine all CC antineutrino cross sections from the neutrino-induced amplitudes.

Besides, the vector contribution of the matrix elements of the weak CC between N and $N'\pi$ states is related to that of the electromagnetic current $s^\mu_{\mathrm{em}}(0)$,

$$s^\mu_{\mathrm{em}} = \frac{2}{3}\bar{\Psi}_u\gamma^\mu\Psi_u - \frac{1}{3}\bar{\Psi}_d\gamma^\mu\Psi_d - \frac{1}{3}\bar{\Psi}_s\gamma^\mu\Psi_s \tag{14}$$

$$= \frac{1}{6}\bar{\Psi}_q\gamma^\mu\Psi_q - \frac{1}{3}\bar{\Psi}_s\gamma^\mu\Psi_s + \frac{1}{\sqrt{2}}\bar{\Psi}_q\gamma^\mu\frac{\tau^1_0}{\sqrt{2}}\Psi_q. \tag{15}$$

The matrix elements of the isovector part (τ^1_0) are related to those of $j_{\mathrm{cc}\pm}$, while the first two terms are isoscalar operators. One easily finds

$$\frac{1}{\cos\theta_C}\langle p\pi^+|V^\mu_{\mathrm{cc}+}(0)|p\rangle = \sqrt{2}\langle n\pi^0|s^\mu_{\mathrm{em}}(0)|n\rangle + \langle p\pi^-|s^\mu_{\mathrm{em}}(0)|n\rangle, \tag{16}$$

$$\frac{1}{\cos\theta_C}\langle n\pi^+|V^\mu_{\mathrm{cc}+}(0)|n\rangle = \sqrt{2}\langle p\pi^0|s^\mu_{\mathrm{em}}(0)|p\rangle - \langle p\pi^-|s^\mu_{\mathrm{em}}(0)|n\rangle. \tag{17}$$

C. Model for the $WN \to N'\pi$ reaction

1. SU(2) nonlinear σ model

Let us start with the effective Lagrangian of the SU(2) nonlinear σ model. It implements the pattern of spontaneous chiral symmetry breaking of QCD, and it is given by

$$\mathcal{L}_{N\pi} = \bar{\Psi}\mathrm{i}\gamma^\mu[\partial_\mu + \mathcal{V}_\mu]\Psi - M\bar{\Psi}\Psi + g_A\bar{\Psi}\gamma^\mu\gamma_5\mathcal{A}_\mu\Psi + \frac{1}{2}\mathrm{Tr}[\partial_\mu U^\dagger\partial^\mu U], \tag{18}$$

where

$$\Psi = \begin{pmatrix}p\\ n\end{pmatrix}$$

is the nucleon field. The fields $\mathcal{V}_\mu$ and $\mathcal{A}_\mu$ are given in terms of the matrix field ξ derived from the pion fields[5] $\vec{\phi}$,

[5]We use a convention such that $\phi = (\phi_x - \mathrm{i}\phi_y)/\sqrt{2}$ creates a π^- from the vacuum or annihilates a π^+, and the ϕ_z field creates or annihilates a π^0.

$$\mathcal{V}_\mu = \frac{1}{2}(\xi\partial_\mu\xi^\dagger + \xi^\dagger\partial_\mu\xi),$$
$$\mathcal{A}_\mu = \frac{\mathrm{i}}{2}(\xi\partial_\mu\xi^\dagger - \xi^\dagger\partial_\mu\xi). \tag{19}$$

The pions $\vec{\phi}$ are the Goldstone bosons associated with the spontaneous breaking of the $SU(2)_V \times SU(2)_A$ chiral symmetry. We describe their dynamics in terms of 2×2 matrix field U given by

$$U = \frac{f_\pi}{\sqrt{2}} e^{\mathrm{i}\vec{\tau}\cdot\vec{\phi}/f_\pi} = \frac{f_\pi}{\sqrt{2}}\xi^2, \tag{20}$$

with $f_\pi \simeq 93$ MeV the pion weak decay constant. The matrix field

$$\xi = e^{\mathrm{i}\vec{\tau}\cdot\vec{\phi}/(2f_\pi)} \tag{21}$$

transforms under $SU(2)_V \times SU(2)_A$ as

$$\xi \overset{SU(2)_V}{\Rightarrow} T_V \xi T_V^\dagger, \qquad \xi \overset{SU(2)_A}{\Rightarrow} T_A^\dagger \xi \Lambda^\dagger = \Lambda \xi T_A^\dagger, \tag{22}$$

where $T_V = \exp(-\mathrm{i}\vec{\tau}\cdot\vec{\theta}_V)/2$ and $T_A = \exp(-\mathrm{i}\vec{\tau}\cdot\vec{\theta}_A)/2$ are global transformations belonging to $SU(2)_V$ and $SU(2)_A$, respectively. As for $\Lambda = \exp(-\mathrm{i}\vec{\tau}\cdot\vec{\theta}_\Lambda)/2$, it is a unitary matrix field that depends on the axial transformation T_A and the $\vec{\phi}$ Goldstone boson fields.

On the other hand, the nucleon field, Ψ, transforms as

$$\Psi \overset{SU(2)_V}{\Rightarrow} T_V \Psi, \qquad \Psi \overset{SU(2)_A}{\Rightarrow} \Lambda\Psi. \tag{23}$$

Each term of the effective Lagrangian of Eq. (18) is separately invariant under the chiral group $SU(2)_V \times SU(2)_A$. This is why one can introduce an axial nucleon coupling $g_A \neq 1$ in the model without violating chiral symmetry. We will use $g_A = 1.26$ throughout this work.

Explicit $SU(2)_A$ breaking terms are included in the model as

$$m_\pi^2 \frac{f_\pi}{\sqrt{2}} \frac{1}{2}\,\mathrm{Tr}(U + U^\dagger - \sqrt{2}f_\pi) \tag{24}$$

to give mass to the pions. Neglecting $\mathcal{O}(1/f_\pi^4)$, the effective Lagrangian of Eqs. (18) and (24) reads

$$\mathcal{L} = \bar{\Psi}[\mathrm{i}\not{\partial} - M]\Psi + \frac{1}{2}\partial_\mu\vec{\phi}\partial^\mu\vec{\phi} - \frac{1}{2}m_\pi^2\vec{\phi}^2 + \mathcal{L}_{\mathrm{int}}^\sigma, \tag{25}$$

$$\begin{aligned}\mathcal{L}_{\mathrm{int}}^\sigma = {}& \frac{g_A}{f_\pi}\bar{\Psi}\gamma^\mu\gamma_5\frac{\vec{\tau}}{2}(\partial_\mu\vec{\phi})\Psi - \frac{1}{4f_\pi^2}\bar{\Psi}\gamma_\mu\vec{\tau}(\vec{\phi}\times\partial^\mu\vec{\phi})\Psi \\ & - \frac{1}{6f_\pi^2}(\vec{\phi}^2\partial_\mu\vec{\phi}\partial^\mu\vec{\phi} - (\vec{\phi}\partial_\mu\vec{\phi})(\vec{\phi}\partial^\mu\vec{\phi})) \\ & + \frac{m_\pi^2}{24f_\pi^2}(\vec{\phi}^2)^2 - \frac{g_A}{6f_\pi^3}\bar{\Psi}\gamma^\mu\gamma_5\Big[\vec{\phi}^2\frac{\vec{\tau}}{2}\partial_\mu\vec{\phi} \\ & - (\vec{\phi}\partial_\mu\vec{\phi})\frac{\vec{\tau}}{2}\vec{\phi}\Big]\Psi + \mathcal{O}\Big(\frac{1}{f_\pi^4}\Big).\end{aligned} \tag{26}$$

In contrast to the linear σ model, the coupling between the p and n and the pions is of the pseudovector type. Writing the coupling constant in the usual way as $g_{\pi NN}/2M = f/m_\pi$, we recover the Goldberger-Treiman relation

$$f = \frac{m_\pi}{2f_\pi}g_A, \tag{27}$$

which phenomenologically is satisfied at the level of 5%.

The vector and axial currents that we derive from the Lagrangian in Eq. (18) and the transformation properties of the fields[6] are given by

$$\begin{aligned}\vec{V}^\mu = {}& \underbrace{\vec{\phi}\times\partial^\mu\vec{\phi}}_{\vec{V}_a^\mu} + \underbrace{\bar{\Psi}\gamma^\mu\frac{\vec{\tau}}{2}\Psi}_{\vec{V}_b^\mu} + \underbrace{\frac{g_A}{2f_\pi}\bar{\Psi}\gamma^\mu\gamma_5(\vec{\phi}\times\vec{\tau})\Psi}_{\vec{V}_c^\mu} \\ & \overbrace{- \frac{1}{4f_\pi^2}\bar{\Psi}\gamma^\mu[\vec{\tau}\vec{\phi}^2 - \vec{\phi}(\vec{\tau}\cdot\vec{\phi})]\Psi - \frac{\vec{\phi}^2}{3f_\pi^2}(\vec{\phi}\times\partial^\mu\vec{\phi})}^{\vec{V}_d^\mu} \\ & + \mathcal{O}\Big(\frac{1}{f_\pi^3}\Big),\end{aligned} \tag{31}$$

[6]For infinitesimal vector and axial transformations, we get from Eq. (22)

$$\vec{\tau}\cdot\vec{\theta}_\Lambda = \frac{\vec{\phi}\times\vec{\tau}}{2f_\pi}\vec{\theta}_A + \mathcal{O}\Big(\frac{1}{f_\pi^3}\Big), \tag{28}$$

$$\begin{aligned}\delta\vec{\phi} &\overset{SU(2)_V}{=} (\vec{\theta}_V\times\vec{\phi}) + \mathcal{O}(1/f_\pi^3), \\ \delta\vec{\phi} &\overset{SU(2)_A}{=} f_\pi\vec{\theta}_A + (\vec{\phi}(\vec{\phi}\cdot\vec{\theta}_A) - \vec{\theta}_A\vec{\phi}^2)/(3f_\pi) + \mathcal{O}(1/f_\pi^3),\end{aligned} \tag{29}$$

$$\begin{aligned}\delta\Psi &\overset{SU(2)_V}{=} -\mathrm{i}\frac{\vec{\tau}\cdot\vec{\theta}_V}{2}\Psi, \\ \delta\Psi &\overset{SU(2)_A}{=} -\mathrm{i}\frac{(\vec{\phi}\times\vec{\tau})\cdot\vec{\theta}_A}{4f_\pi}\Psi + \mathcal{O}(1/f_\pi^3),\end{aligned} \tag{30}$$

where $\delta\vec{\phi}$ and $\delta\Psi$ denote the infinitesimal variations of the fields.

$$\vec{A}^{\mu} = \underbrace{f_{\pi}\partial^{\mu}\vec{\phi}}_{\vec{A}_a^{\mu}} + \underbrace{g_A\bar{\Psi}\gamma^{\mu}\gamma_5\frac{\vec{\tau}}{2}\Psi}_{\vec{A}_b^{\mu}} + \underbrace{\frac{1}{2f_{\pi}}\bar{\Psi}\gamma^{\mu}(\vec{\phi}\times\vec{\tau})\Psi}_{\vec{A}_c^{\mu}} + \overbrace{\frac{2}{3f_{\pi}}[\vec{\phi}(\vec{\phi}\cdot\partial^{\mu}\vec{\phi}) - \vec{\phi}^2\partial^{\mu}\vec{\phi}] - \frac{g_A}{4f_{\pi}^2}\bar{\Psi}\gamma^{\mu}\gamma_5[\vec{\tau}\vec{\phi}^2 - \vec{\phi}(\vec{\tau}\cdot\vec{\phi})]\Psi}^{\vec{A}_d^{\mu}} + \mathcal{O}\left(\frac{1}{f_{\pi}^3}\right), \tag{32}$$

and determine the weak transition vertex where the W-boson is absorbed. This is because these currents, up to a factor of $\cos\theta_C$, are the hadronic realization of the electroweak quark current j^{μ}_{cc} for a system of interacting pions and nucleons. Thus, $\vec{A}^{\mu}_a$ and $\vec{V}^{\mu}_a$ account for the W-decay into one and two pions, respectively, while $\vec{A}^{\mu}_b$ and $\vec{V}^{\mu}_b$ provide the WNN vector and axial vector couplings. Besides, $\vec{A}^{\mu}_c$ and $\vec{V}^{\mu}_c$ lead to contact $WNN\pi$ vertices and finally $\vec{A}^{\mu}_d$ and $\vec{V}^{\mu}_d$ either contribute to processes with more than one pion in the final state or provide loop corrections to the leading order amplitude for one pion production.

The overall normalization is fixed by the W^+np vertex

$$\langle p;\vec{p}\,' = \vec{p} + \vec{q}|j^{\alpha}_{\mathrm{cc}+}(0)|n;\vec{p}\rangle = \cos\theta_C\bar{u}(\vec{p}\,')(V^{\alpha}_N(q) - A^{\alpha}_N(q))u(\vec{p}), \tag{33}$$

where the u's are Dirac spinors for the neutron and proton, normalized such that $\bar{u}u = 2M$, and vector and axial nucleon currents are given by

$$V^{\alpha}_N(q) = 2\times\left(F_1^V(q^2)\gamma^{\alpha} + \mathrm{i}\mu_V\frac{F_2^V(q^2)}{2M}\sigma^{\alpha\nu}q_{\nu}\right),$$
$$A^{\alpha}_N(q) = G_A(q^2)\times\left(\gamma^{\alpha}\gamma_5 + \frac{\not{q}}{m_{\pi}^2 - q^2}q^{\alpha}\gamma_5\right), \tag{34}$$

all form factors being real thanks to invariance under time reversal. Invariance under G-parity has been assumed to discard a term of the form $(p^{\mu} + p'^{\mu})\gamma_5$, and we have only considered the pion pole-contribution in the pseudoscalar form factor. Isospin symmetry relates the vector form factors to the electromagnetic ones[7]

$$F_1^V(q^2) = \frac{1}{2}(F_1^p(q^2) - F_1^n(q^2)),$$
$$\mu_V F_2^V(q^2) = \frac{1}{2}(\mu_p F_2^p(q^2) - \mu_n F_2^n(q^2)), \tag{36}$$

[7]We use the parameterization of Galster and collaborators [22]

$$F_1^N = \frac{G_E^N + \tau G_M^N}{1+\tau}, \qquad \mu_N F_2^N = \frac{G_M^N - G_E^N}{1+\tau},$$
$$G_E^p = \frac{G_M^p}{\mu_p} = \frac{G_M^n}{\mu_n} = -(1+\lambda_n\tau)\frac{G_E^n}{\mu_n\tau} = \left(\frac{1}{1-q^2/M_D^2}\right)^2, \tag{35}$$

with $\tau = -q^2/4M^2$, $M_D = 0.843$ GeV, $\mu_p = 2.792\,847$, $\mu_n = -1.913\,043$, and $\lambda_n = 5.6$.

and the axial form factor is given by [23]

$$G_A(q^2) = \frac{g_A}{(1-q^2/M_A^2)^2}, \qquad g_A = 1.26, \quad M_A = 1.05\ \mathrm{GeV}. \tag{37}$$

Thus, one realizes that, up to an overall $-\sqrt{2}\cos\theta_C$ factor, the $+1$ spherical component[8] ($[A^{\mu}_b]_{+1} = -([A^{\mu}_b]_x + \mathrm{i}[A^{\mu}_b]_y)/\sqrt{2}$) of $\vec{A}^{\mu}_b$ gives the axial vector contribution, at $q^2 = 0$, of the $W^+n\to p$ weak transition. Besides, $-\sqrt{2}[A^{\mu}_a]_{+1}$ and the πNN coupling in $\mathcal{L}^{\sigma}_{\mathrm{int}}$ lead to the $q^{\mu}\gamma_5$ term in Eq. (34). Analogously, $-\sqrt{2}\cos\theta_C[V^{\mu}_b]_{+1}$ provides the Dirac part of the vector contribution, at $q^2 = 0$, of the $W^+n\to p$ weak transition. The magnetic part in Eq. (34) is not provided by the nonlinear sigma model constructed here which assumes structureless nucleons.

From the above discussion, we conclude that $-\sqrt{2}\cos\theta_C([V^{\mu}]_{+1} - [A^{\mu}]_{+1})$ provides the W^+- absorption vertex, with the appropriate normalization, in the $\langle N'\pi|j^{\mu}_{\mathrm{cc}+}(0)|N\rangle$ matrix element. We will improve on that by including the q^2 dependence induced by the form factors in Eq. (34) and adding the magnetic contribution (F_2^V term) to the vector part of the $W^+N\to N$ amplitude.

2. The $WN\Delta$ and $N\Delta\pi$ vertices

At intermediate energies, the weak excitation of the $\Delta(1232)$ resonance and its subsequent decay into $N\pi$ dominates the $WN\to N'\pi$ reaction. A convenient parametrization for the $W^+n\to\Delta^+$ hadron matrix element is the following: [9]

$$\langle\Delta^+;p_{\Delta} = p+q|j^{\mu}_{\mathrm{cc}+}(0)|n;p\rangle = \bar{u}_{\alpha}(\vec{p}_{\Delta})\Gamma^{\alpha\mu}(p,q)\times u(\vec{p})\cos\theta_C, \tag{39}$$

where

[8]Note,

$$-\sqrt{2}\tau_{+1}|n\rangle = (\tau_x + \mathrm{i}\tau_y)|n\rangle = 2|p\rangle. \tag{38}$$

$$\Gamma^{\alpha\mu}(p,q) = \left[\frac{C_3^V}{M}(g^{\alpha\mu}\not{q} - q^\alpha\gamma^\mu) + \frac{C_4^V}{M^2}(g^{\alpha\mu}q\cdot p_\Delta - q^\alpha p_\Delta^\mu) + \frac{C_5^V}{M^2}(g^{\alpha\mu}q\cdot p - q^\alpha p^\mu) + C_6^V g^{\alpha\mu}\right]\gamma_5 + \left[\frac{C_3^A}{M}(g^{\alpha\mu}\not{q} - q^\alpha\gamma^\mu) + \frac{C_4^A}{M^2}(g^{\alpha\mu}q\cdot p_\Delta - q^\alpha p_\Delta^\mu) + C_5^A g^{\alpha\mu} + \frac{C_6^A}{M^2}q^\mu q^\alpha\right], \quad p_\Delta = p+q, \tag{40}$$

with $C_{3,4,5,6}^V$ and $C_{3,4,5,6}^A$ scalar and real vector and axial form factors, which depend on q^2. Besides, u_α is a Rarita-Schwinger spinor for the Δ^+. The $N\Delta\pi$ coupling is given by

$$\mathcal{L}_{\pi N\Delta} = \frac{f^*}{m_\pi}\bar{\Psi}_\mu \vec{T}^\dagger(\partial^\mu\vec{\phi})\Psi + \text{h.c.} \tag{41}$$

where Ψ_μ is a Rarita-Schwinger $J^\pi = 3/2^+$ field, $\vec{T}^\dagger$ is the isospin transition operator[9] from isospin 1/2 to 3/2, and $f^* = 2.13 \times f = 2.14$. The Goldberger-Treiman relation implies here[10]

$$C_5^A(0) = \sqrt{\frac{2}{3}}\frac{f_\pi}{m_\pi}f^* \sim 1.15. \tag{42}$$

For the Δ-propagator $G^{\mu\nu}(p_\Delta)$, we use in momentum space

$$G^{\mu\nu}(p_\Delta) = \frac{P^{\mu\nu}(p_\Delta)}{p_\Delta^2 - M_\Delta^2 + iM_\Delta\Gamma_\Delta}, \tag{43}$$

with M_Δ the resonance mass ($\sim$ 1232 MeV), $P^{\mu\nu}$ the spin 3/2 projection operator

$$P^{\mu\nu}(p_\Delta) = -(\not{p}_\Delta + M_\Delta)\left[g^{\mu\nu} - \frac{1}{3}\gamma^\mu\gamma^\nu - \frac{2}{3}\frac{p_\Delta^\mu p_\Delta^\nu}{M_\Delta^2} + \frac{1}{3}\frac{p_\Delta^\mu\gamma^\nu - p_\Delta^\nu\gamma^\mu}{M_\Delta}\right], \tag{44}$$

and Γ_Δ the resonance width in its rest frame, given by

$$\Gamma_\Delta(s) = \frac{1}{6\pi}\left(\frac{f^*}{m_\pi}\right)^2\frac{M}{\sqrt{s}}\left[\frac{\lambda^{1/2}(s,m_\pi^2,M^2)}{2\sqrt{s}}\right]^3 \times \Theta(\sqrt{s} - M - m_\pi), \qquad s = p_\Delta^2, \tag{45}$$

with $\lambda(x,y,z) = x^2 + y^2 + z^2 - 2xy - 2xz - 2yz$ and Θ the step function, as deduced from the Lagrangian of Eq. (41).

The determination of the form factors follows from general principles and experimental results. The imposition of the conserved vector current hypothesis implies $C_6^V = 0$. The other three vector form factors are then given in terms of the isovector electromagnetic form factors in the $p - \Delta^+$ transition. The analysis of photo and electroproduction data of Δ is done in terms of multipole amplitudes [24]. Most of the previous papers on neutrino production [13,17,18] assume M_{1^+} dominance[11] of the electroproduction amplitude, which implies $C_5^V = 0$ and a relation between C_4^V and C_3^V. Here, we take advantage of the recent work of Lalakulich, Paschos and Piranishvili and improve on that by including the effect of the subdominant multipoles [19]

$$C_3^V = \frac{2.13}{(1 - q^2/M_V^2)^2}\times\frac{1}{1 - \frac{q^2}{4M_V^2}}, \qquad C_4^V = \frac{-1.51}{(1 - q^2/M_V^2)^2}\times\frac{1}{1 - \frac{q^2}{4M_V^2}}, \qquad C_5^V = \frac{0.48}{(1 - q^2/M_V^2)^2}\times\frac{1}{1 - \frac{q^2}{0.776M_V^2}}, \tag{46}$$

with $M_V = 0.84$ GeV. Among the axial form factors the most important contribution comes from C_5^A, whose numerical value is related to the pseudoscalar form factor C_6^A by partial conservation of axial current (PCAC). Since there are no other theoretical constraints for $C_3^A(q^2)$, $C_4^A(q^2)$, and $C_5^A(q^2)/C_5^A(0)$, they have to be fitted to neutrino scattering data. The available information comes mainly from two bubble chamber experiments, ANL [20,26,27] and BNL [21,28]. We adopt the Adler model [8], as the ANL and BNL analyses did, where

$$C_4^A(q^2) = -\frac{C_5^A(q^2)}{4}, \qquad C_3^A(q^2) = 0, \tag{47}$$

and for $C_{5,6}^A$ we shall use [16]

$$C_5^A(q^2) = \frac{1.2}{(1 - q^2/M_{A\Delta}^2)^2}\times\frac{1}{1 - \frac{q^2}{3M_{A\Delta}^2}}, \qquad C_6^A(q^2) = C_5^A(q^2)\frac{M^2}{m_\pi^2 - q^2}, \quad \text{with} \quad M_{A\Delta} = 1.05 \text{ GeV}. \tag{48}$$

The value for C_4^A was found to give a small contribution to the cross section and setting the C_3^A form factor to zero is consistent with early dispersion calculations [8,29] and recent lattice QCD results [30]. Note that the contribution to the differential cross section of the C_6^A term will be always proportional to the outgoing lepton mass.

Isospin symmetry implies that the transition matrix element $W^+p \to \Delta^{++}$ is a factor $\sqrt{3}$ bigger than the $W^+n \to \Delta^+$ one discussed above.

[9] It is a vector under isospin rotations and its Wigner-Eckart irreducible matrix element is taken to be one.

[10] Note that the C_5^A sign is quoted incorrectly in Ref. [9] (see comment in Ref. [10]).

[11] Recent data determine the contribution from the electric multipole E_{1^+}/M_{1^+} to be $\sim -2.5\%$ and from the scalar multipole $S_{1^+}/M_{1^+} \sim -2.5\%$ [25].

For the weak transition $\Delta \to N$, we have

$$\langle N;p'|j^{\mu}_{\mathrm{cc}+}(0)|\Delta;p_\Delta = p'-q\rangle = \langle \Delta;p_\Delta = p'-q|j^{\mu}_{\mathrm{cc}-}(0)|N;p'\rangle^* \quad (49)$$

$$= -\frac{(\frac{1}{2},1,\frac{3}{2}|t_N,-1,t_\Delta)}{(\frac{1}{2},1,\frac{3}{2}|-\frac{1}{2},1,\frac{1}{2})}\{\bar{u}_\alpha(\vec{p}_\Delta=\vec{p}'-\vec{q}) \times \Gamma^{\alpha\mu}(p',-q)u(\vec{p}')\cos\theta_C\}^*, \quad (50)$$

with $(t_1,t_2,t|m_1,m_2,m)$ Clebsch-Gordan coefficients and t_N and t_Δ the nucleon and delta isobar isospin third components, respectively.

3. Explicit expressions for the $\langle p\pi^+|j^{\mu}_{\mathrm{cc}+}(0)|p\rangle$ and $\langle n\pi^+|j^{\mu}_{\mathrm{cc}+}(0)|n\rangle$ amplitudes

In this subsection, we give explicit expressions for the $\langle p\pi^+|j^{\mu}_{\mathrm{cc}+}(0)|p\rangle$ and $\langle n\pi^+|j^{\mu}_{\mathrm{cc}+}(0)|n\rangle$ amplitudes, which we will denote by $(j^{\mu}_{\mathrm{cc}+})_{p\pi^+}$ and $(j^{\mu}_{\mathrm{cc}+})_{n\pi^+}$, respectively. All $\langle N'\pi|j^{\mu}_{\mathrm{cc}\pm}(0)|N\rangle$ matrix elements can be expressed in terms of these two amplitudes (Sec. II B). The model consists of seven Feynman diagrams, depicted in Fig. 2, constructed out of the $W^+N\to N$, $W^+N\to\Delta$, $W^+N\to N\pi$, and the contact $W^+\pi\to\pi$ weak transition vertices [Eqs. (31)–(33) and (39)] and the πNN, $\pi\pi NN$ [Eq. (26)], and $\pi N\Delta$ [Eq. (41)] couplings, discussed in Secs. II C 1 and II C 2. Since we have included a q^2 dependence $[F_1^V(q^2)]$ on the Dirac part of the vector WNN vertex and to preserve vector current conservation, we also include form factors in the V_a^μ and V_c^μ weak operators. Those are the $F_{\mathrm{PF}}(q^2)$ and $F^V_{\mathrm{CT}}(q^2)$ form factors that appear in the pion-in-flight (PF) and contact term (CT) contributions below. This partially accounts for the nucleon structure.

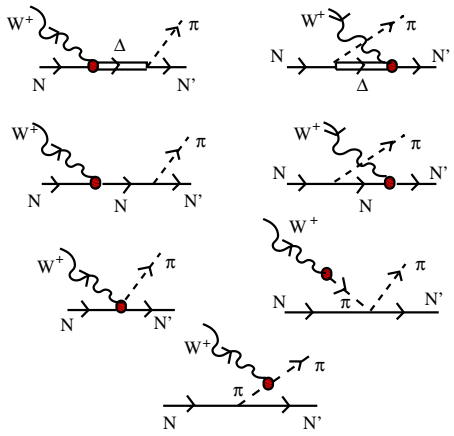

FIG. 2 (color online). Model for the $W^+N\to N'\pi$ reaction. It consists of seven diagrams: Direct and crossed $\Delta(1232)$- (first row) and nucleon (second row) pole terms, contact and pion pole contribution (third row) and finally the pion-in-flight term. Throughout this work, we will denote these contributions by ΔP, $C\Delta P$, NP, CNP, CT, PP, and PF, respectively. The circle in the diagrams stands for the weak transition vertex.

We do not include loop corrections. This model is an extension of that developed in Ref. [31] for the $eN\to e'N\pi$ reaction, though there exist some minor differences related to the used form factors and a nonrelativistic reduction was performed in Ref. [31].

The amplitudes read,

$$j^{\mu}_{\mathrm{cc}+}|_{\Delta P} = \mathrm{i}C^{\Delta P}\frac{f^*}{m_\pi}\sqrt{3}\cos\theta_C\frac{k_\pi^\alpha}{p_\Delta^2-M_\Delta^2+iM_\Delta\Gamma_\Delta}\bar{u}(\vec{p}')P_{\alpha\beta}(p_\Delta)\Gamma^{\beta\mu}(p,q)u(\vec{p}),\quad p_\Delta=p+q,\quad \text{and}\quad C^{\Delta P}=\begin{pmatrix}1 & \text{for } p\pi^+\\ 1/3 & \text{for } n\pi^+\end{pmatrix},$$

$$j^{\mu}_{\mathrm{cc}+}|_{C\Delta P} = \mathrm{i}C^{C\Delta P}\frac{f^*}{m_\pi}\frac{1}{\sqrt{3}}\cos\theta_C\frac{k_\pi^\beta}{p_\Delta^2-M_\Delta^2+iM_\Delta\Gamma_\Delta}\bar{u}(\vec{p}')\hat{\Gamma}^{\mu\alpha}(p',q)P_{\alpha\beta}(p_\Delta)u(\vec{p}),$$

$$p_\Delta=p'-q,\quad \text{and}\quad C^{C\Delta P}=\begin{pmatrix}1 & \text{for } p\pi^+\\ 3 & \text{for } n\pi^+\end{pmatrix},\quad \hat{\Gamma}^{\mu\alpha}(p',q)=\gamma^0[\Gamma^{\alpha\mu}(p',-q)]^\dagger\gamma^0,$$

$$j^{\mu}_{\mathrm{cc}+}|_{\mathrm{NP}} = -\mathrm{i}C^{\mathrm{NP}}\frac{g_A}{\sqrt{2}f_\pi}\cos\theta_C\bar{u}(\vec{p}')\not{k}_\pi\gamma_5\frac{\not{p}+\not{q}+M}{(p+q)^2-M^2+i\epsilon}[V_N^\mu(q)-A_N^\mu(q)]u(\vec{p}),\quad C^{\mathrm{NP}}=\begin{pmatrix}0 & \text{for } p\pi^+\\ 1 & \text{for } n\pi^+\end{pmatrix},$$

$$j^{\mu}_{\mathrm{cc}+}|_{\mathrm{CNP}} = -\mathrm{i}C^{\mathrm{CNP}}\frac{g_A}{\sqrt{2}f_\pi}\cos\theta_C\bar{u}(\vec{p}')[V_N^\mu(q)-A_N^\mu(q)]\frac{\not{p}'-\not{q}+M}{(p'-q)^2-M^2+i\epsilon}\not{k}_\pi\gamma_5 u(\vec{p}),\quad C^{\mathrm{CNP}}=\begin{pmatrix}1 & \text{for } p\pi^+\\ 0 & \text{for } n\pi^+\end{pmatrix},$$

$$j^{\mu}_{\mathrm{cc}+}|_{\mathrm{CT}} = -\mathrm{i}C^{\mathrm{CT}}\frac{1}{\sqrt{2}f_\pi}\cos\theta_C\bar{u}(\vec{p}')\gamma^\mu(g_AF^V_{\mathrm{CT}}(q^2)\gamma_5-F_\rho((q-k_\pi)^2))u(\vec{p}),\quad C^{\mathrm{CT}}=\begin{pmatrix}1 & \text{for } p\pi^+\\ -1 & \text{for } n\pi^+\end{pmatrix},$$

$$j^{\mu}_{\mathrm{cc}+}|_{\mathrm{PP}} = -\mathrm{i}C^{\mathrm{PP}}F_\rho((q-k_\pi)^2)\frac{1}{\sqrt{2}f_\pi}\cos\theta_C\frac{q^\mu}{q^2-m_\pi^2}\bar{u}(\vec{p}')\not{q}u(\vec{p}),\quad C^{\mathrm{PP}}=\begin{pmatrix}1 & \text{for } p\pi^+\\ -1 & \text{for } n\pi^+\end{pmatrix},$$

$$j^{\mu}_{\mathrm{cc}+}|_{\mathrm{PF}} = -\mathrm{i}C^{\mathrm{PF}}F_{\mathrm{PF}}(q^2)\frac{g_A}{\sqrt{2}f_\pi}\cos\theta_C\frac{(2k_\pi-q)^\mu}{(k_\pi-q)^2-m_\pi^2}2M\bar{u}(\vec{p}')\gamma_5u(\vec{p}),\quad C^{\mathrm{PF}}=\begin{pmatrix}1 & \text{for } p\pi^+\\ -1 & \text{for } n\pi^+\end{pmatrix}, \quad (51)$$

where ΔP, $C\Delta P$, NP, CNP, and PP stand for delta pole, crossed delta pole, nucleon pole, crossed nucleon pole, and pion pole contributions, respectively.

Note that in the PF (PP) term the weak transition is purely driven by the vector (axial) CC. The contribution proportional to g_A in the CT diagram is the one due to the vector weak transition. We impose

$$F_{\rm PF}(q^2) = F_{\rm CT}^V(q^2) = 2F_1^V(q^2) = F_1^p - F_1^n \tag{52}$$

to preserve conservation of vector current, as we required for the ΔN weak transition. Besides, we have included a form factor

$$F_\rho(t) = \frac{1}{1 - t/m_\rho^2}, \qquad m_\rho = 0.7758\ \text{GeV} \tag{53}$$

in the PP term to account for the ρ-meson dominance of the $\pi\pi NN$ coupling. To preserve PCAC, the same form factor has been included in the CT axial contribution.

In the pion-in-flight term, we have the coupling πNN with a virtual pion. It is usual in the literature to use a form factor to account for the off-shellness of the pion. To preserve vector current conservation, if one includes this form factor in this term, one should also multiply by the same factor the CT term and the NP and CNP F_1^V contributions. This was the adopted scheme in the study of the $eN \to e'N\pi$ reaction carried out in Ref. [31], where the induced changes by its inclusion turned out to be moderately small. In the weak pion production case, there are more important sources of uncertainties[12] and the existing measurements are poorer. This work being one of the first studies of weak pion production where background terms are added to the dominant Δ contribution, and for the sake of simplicity, we do not include this form factor.

The average and sum over the initial and final spins in Eq. (4) is readily done thanks to

$$\begin{aligned}&\bar{\sum_{\rm spins}}\ \bar{u}(\vec{p}\,')\mathcal{S}^\mu u(\vec{p})[\bar{u}(\vec{p}\,')\mathcal{S}^\sigma u(\vec{p})]^* \\ &\quad = \frac{1}{2}\,\mathrm{Tr}((\not{p}' + M)\mathcal{S}^\mu(\not{p} + M)\gamma^0\mathcal{S}^{\dagger\sigma}\gamma^0),\end{aligned} \tag{54}$$

where the spin dependence of the Dirac's spinors is understood and $\mathcal{S}^\mu$ is a matrix in the Dirac's space for each value of the Lorentz index μ.

III. NC NEUTRINO- AND ANTINEUTRINO-INDUCED REACTIONS

The unpolarized differential cross section in the LAB frame for the process

$$\nu_l(k) + N(p) \to \nu_l(k') + N(p') + \pi(k_\pi) \tag{55}$$

reads

$$\begin{aligned}\frac{d^5\sigma_{\nu\nu}}{d\Omega(\hat{k}')dE'd\Omega(\hat{k}_\pi)} &= \frac{|\vec{k}'|}{|\vec{k}|}\frac{G^2}{16\pi^2} \\ &\quad\times \int_0^{+\infty}\frac{dk_\pi k_\pi^2}{E_\pi}L_{\mu\sigma}^{(\nu)}(W_{{\rm NC}\pi}^{\mu\sigma})^{(\nu)},\end{aligned} \tag{56}$$

with $\vec{k}'$, $E' = |\vec{k}'|$ the LAB outgoing neutrino momentum and energy. The leptonic tensor is given in Eq. (3), and it is now orthogonal to $q^\mu = (k - k')^\mu$ for massless neutrinos, i.e, $L_{\mu\sigma}^{(\nu)}q^\mu = L_{\mu\sigma}^{(\nu)}q^\sigma = 0$.

The hadronic tensor reads

$$\begin{aligned}(W_{{\rm NC}\pi}^{\mu\sigma})^{(\nu)} &= \frac{1}{4M}\bar{\sum_{\rm spins}}\int\frac{d^3p'}{(2\pi)^3}\frac{1}{2E_N'}\delta^4(p' + k_\pi - q - p) \\ &\quad\times\langle N'\pi|j_{\rm nc}^\mu(0)|N\rangle\langle N'\pi|j_{\rm nc}^\sigma(0)|N\rangle^*,\end{aligned} \tag{57}$$

where the neutral current at the quark level is

$$\begin{aligned}j_{\rm nc}^\mu &= \bar{\Psi}_u\gamma^\mu\left(1 - \frac{8}{3}\sin^2\theta_W - \gamma_5\right)\Psi_u \\ &\quad - \bar{\Psi}_d\gamma^\mu\left(1 - \frac{4}{3}\sin^2\theta_W - \gamma_5\right)\Psi_d \\ &\quad - \bar{\Psi}_s\gamma^\mu\left(1 - \frac{4}{3}\sin^2\theta_W - \gamma_5\right)\Psi_s \\ &= \bar{\Psi}_q\gamma^\mu(1 - \gamma_5)\tau_0^1\Psi_q - 4\sin^2\theta_W s_{\rm em}^\mu \\ &\quad - \bar{\Psi}_s\gamma^\mu(1 - \gamma_5)\Psi_s,\end{aligned} \tag{58}$$

where θ_W is the Weinberg angle ($\sin^2\theta_W = 0.231$).

Both lepton and hadron tensors are independent of the neutrino lepton family, and therefore the cross section for the reaction of Eq. (55) is the same for electron, muon, or tau incident neutrinos. For antineutrino-induced reactions we have, besides the relation of Eq. (8) for the leptonic tensor,

$$(W_{{\rm NC}\pi}^{\mu\sigma})^{(\bar{\nu})} = (W_{{\rm NC}\pi}^{\mu\sigma})^{(\nu)}. \tag{59}$$

As discussed above for the CC-induced process, Lorentz invariance here also restricts the ϕ_π dependence, and the NC differential cross section can be written as in Eq. (7). This ϕ_π dependence has been carefully studied in Ref. [32] as a potential tool to distinguish τ-neutrinos from antineutrinos, below the τ-production threshold, but above the pion production one.

The NC can be expressed as

$$\begin{aligned}j_{\rm nc}^\mu &= \bar{\Psi}_q\gamma^\mu(1 - 2\sin^2\theta_W - \gamma_5)\tau_0^1\Psi_q - 4\sin^2\theta_W s_{\rm em,IS}^\mu \\ &\quad - \bar{\Psi}_s\gamma^\mu(1 - \gamma_5)\Psi_s,\end{aligned} \tag{60}$$

where the isoscalar part of the electromagnetic current is given by

$$s_{\rm em,IS}^\mu = \frac{1}{6}\bar{\Psi}_q\gamma^\mu\Psi_q - \frac{1}{3}\bar{\Psi}_s\gamma^\mu\Psi_s. \tag{61}$$

[12]For instance: partial knowledge of the Δ resonance form factors, possible pion off-shell effects in the weak transition vertex of the PP diagram, etc.…

Isospin symmetry relates the matrix elements of the isovector part (τ_0^1 term) of $j^\mu_{\rm nc}$ with those of the vector ($V^\mu_{{\rm cc}+}$) and axial ($A^\mu_{{\rm cc}+}$) part of the current $j^\mu_{{\rm cc}+}(=V^\mu_{{\rm cc}+}-A^\mu_{{\rm cc}+})$,

$$\begin{aligned}
&\langle p\pi^0|\bar\Psi_q\gamma^\mu(1-2\sin^2\theta_W-\gamma_5)\tau_0^1\Psi_q|p\rangle\\
&\quad=\frac{1}{\sqrt{2}\cos\theta_C}\{(1-2\sin^2\theta_W)[\langle p\pi^+|V^\mu_{{\rm cc}+}(0)|p\rangle\\
&\qquad+\langle n\pi^+|V^\mu_{{\rm cc}+}(0)|n\rangle]-[\langle p\pi^+|A^\mu_{{\rm cc}+}(0)|p\rangle\\
&\qquad+\langle n\pi^+|A^\mu_{{\rm cc}+}(0)|n\rangle]\},
\end{aligned}\tag{62}$$

$$\begin{aligned}
&\langle n\pi^+|\bar\Psi_q\gamma^\mu(1-2\sin^2\theta_W-\gamma_5)\tau_0^1\Psi_q|p\rangle\\
&\quad=-\frac{1}{\cos\theta_C}\{(1-2\sin^2\theta_W)[\langle p\pi^+|V^\mu_{{\rm cc}+}(0)|p\rangle\\
&\qquad-\langle n\pi^+|V^\mu_{{\rm cc}+}(0)|n\rangle]-[\langle p\pi^+|A^\mu_{{\rm cc}+}(0)|p\rangle\\
&\qquad-\langle n\pi^+|A^\mu_{{\rm cc}+}(0)|n\rangle]\},
\end{aligned}\tag{63}$$

$$\begin{aligned}
&\langle n\pi^0|\bar\Psi_q\gamma^\mu(1-2\sin^2\theta_W-\gamma_5)\tau_0^1\Psi_q|n\rangle\\
&\quad=\langle p\pi^0|\bar\Psi_q\gamma^\mu(1-2\sin^2\theta_W-\gamma_5)\tau_0^1\Psi_q|p\rangle,\\
&\langle p\pi^-|\bar\Psi_q\gamma^\mu(1-2\sin^2\theta_W-\gamma_5)\tau_0^1\Psi_q|n\rangle\\
&\quad=-\langle n\pi^+|\bar\Psi_q\gamma^\mu(1-2\sin^2\theta_W-\gamma_5)\tau_0^1\Psi_q|p\rangle.
\end{aligned}\tag{64}$$

For the isoscalar part of the electromagnetic current we have

$$\begin{aligned}
\langle n\pi^+|s^\mu_{\rm em,IS}|p\rangle&=\langle p\pi^-|s^\mu_{\rm em,IS}|n\rangle=\sqrt{2}\langle p\pi^0|s^\mu_{\rm em,IS}|p\rangle\\
&=-\sqrt{2}\langle n\pi^0|s^\mu_{\rm em,IS}|n\rangle,
\end{aligned}\tag{65}$$

with

$$\langle p\pi^0|s^\mu_{\rm em,IS}|p\rangle=-\frac{\langle n\pi^0|s^\mu_{\rm em}(0)|n\rangle-\langle p\pi^0|s^\mu_{\rm em}(0)|p\rangle}{2}.\tag{66}$$

To compute $\langle N\pi^0|s^\mu_{\rm em}(0)|N\rangle$, we derive the electromagnetic current associated with the Lagrangian of the SU(2) nonlinear σ model of Eq. (25),

$$\begin{aligned}
s^\mu_{\rm em}=\bar\Psi\gamma^\mu\left(\frac{1+\tau_z}{2}\right)\Psi+\frac{ig_A}{2f_\pi}\bar\Psi\gamma^\mu\gamma_5(\tau^1_{-1}\phi^\dagger+\tau^1_{+1}\phi)\Psi\\
+i(\phi^\dagger\partial^\mu\phi-\phi\partial^\mu\phi^\dagger)+\cdots
\end{aligned}\tag{67}$$

where we have only kept those terms contributing to one pion production in the absence of chiral loop corrections. Thus, within our framework, the model for the $\gamma N\to\pi N$ reaction would consist of direct and crossed nucleon pole, contact, and pion-in-flight terms. As we did for the CC driven processes, such a model should be supplemented by including (i) the q^2 dependence induced by the Dirac $F_1^{p,n}$ form factors, (ii) the magnetic contribution in the γNN vertex, and (iii) the direct and crossed $\Delta(1232)$ pole terms [31]. However, the Δ-resonance diagrams cannot contribute to the matrix elements of the isoscalar part of the electromagnetic current. Besides, from Eq. (67) we see that neither the pion-in-flight nor the contact terms contribute for π^0 photoproduction. Hence, to compute $\langle n\pi^0|s^\mu_{\rm em}(0)|n\rangle-\langle p\pi^0|s^\mu_{\rm em}(0)|p\rangle$, we are just left with the direct and crossed nucleon pole terms

$$\begin{aligned}
&\frac{\langle n\pi^0|s^\mu_{\rm em}(0)|n\rangle-\langle p\pi^0|s^\mu_{\rm em}(0)|p\rangle}{2}\\
&\quad=i\frac{g_A}{2f_\pi}\bar u(\vec p\,')\Big\{\not k_\pi\gamma_5\frac{\not p+\not q+M}{(p+q)^2-M^2+i\epsilon}\\
&\qquad\times\left[F_1^{\rm IS}(q^2)\gamma^\mu+i\mu_{\rm IS}\frac{F_2^{\rm IS}(q^2)}{2M}\sigma^{\mu\nu}q_\nu\right]\\
&\qquad+\left[F_1^{\rm IS}(q^2)\gamma^\mu+i\mu_{\rm IS}\frac{F_2^{\rm IS}(q^2)}{2M}\sigma^{\mu\nu}q_\nu\right]\\
&\qquad\times\frac{\not p'-\not q+M}{(p'-q)^2-M^2+i\epsilon}\not k_\pi\gamma_5\Big\}u(\vec p),
\end{aligned}\tag{68}$$

with

$$\begin{aligned}
F_1^{\rm IS}(q^2)&=\frac{1}{2}(F_1^p(q^2)+F_1^n(q^2)),\\
\mu_{\rm IS}F_2^{\rm IS}(q^2)&=\frac{1}{2}(\mu_pF_2^p(q^2)+\mu_nF_2^n(q^2)).
\end{aligned}\tag{69}$$

Finally, we pay attention to the matrix elements of the isoscalar operator $\bar\Psi_s\gamma^\mu(1-\gamma_5)\Psi_s$ which are sensitive to the strange content of the hadrons. Due to its isoscalar character we have

$$\begin{aligned}
&\langle n\pi^+|(\bar\Psi_s\gamma^\mu(1-\gamma_5)\Psi_s)(0)|p\rangle\\
&\quad=\langle p\pi^-|(\bar\Psi_s\gamma^\mu(1-\gamma_5)\Psi_s)(0)|n\rangle\\
&\quad=\sqrt{2}\langle p\pi^0|(\bar\Psi_s\gamma^\mu(1-\gamma_5)\Psi_s)(0)|p\rangle\\
&\quad=-\sqrt{2}\langle n\pi^0|(\bar\Psi_s\gamma^\mu(1-\gamma_5)\Psi_s)(0)|n\rangle.
\end{aligned}\tag{70}$$

This part of the NC operator can neither lead to $N\Delta$ transitions nor couple to a single pion. Thus, and assuming a model for the $Z^0N\to N'\pi$ reactions similar to that used for the CC driven process, we should consider the contributions of the direct and crossed nucleon pole, the contact, and the pion-in-flight terms to the matrix element of the $\bar\Psi_s\gamma^\mu(1-\gamma_5)\Psi_s$ quark operator. The contribution of the first two terms (NP and CNP) reads

$$\begin{aligned}
&\langle p\pi^0|(\bar\Psi_s\gamma^\mu(1-\gamma_5)\Psi_s)(0)|p\rangle\\
&=-i\frac{g_A}{2f_\pi}\bar u(\vec p\,')\Big\{\not k_\pi\gamma_5\frac{\not p+\not q+M}{(p+q)^2-M^2+i\epsilon}\Big[F_1^s(q^2)\gamma^\mu\\
&\quad+i\mu_s\frac{F_2^s(q^2)}{2M}\sigma^{\mu\nu}q_\nu-G_A^s(q^2)\gamma^\mu\gamma_5-G_P^sq^\mu\gamma_5\Big]\\
&\quad+\Big[F_1^s(q^2)\gamma^\mu+i\mu_s\frac{F_2^s(q^2)}{2M}\sigma^{\mu\nu}q_\nu-G_A^s(q^2)\gamma^\mu\gamma_5\\
&\quad-G_P^sq^\mu\gamma_5\Big]\frac{\not p'-\not q+M}{(p'-q)^2-M^2+i\epsilon}\not k_\pi\gamma_5\Big\}u(\vec p),
\end{aligned}\tag{71}$$

where F_1^s, $\mu_s F_2^s$, G_A^s, and G_P^s are the strange vector and axial nucleon form factors [33]. The pseudoscalar part of the axial current does not contribute to the differential cross section for massless neutrinos, and for the rest of the strange form factors we use the results of fit II of Ref. [34],

$$G_A^s(q^2) = \frac{g_S}{(1 - q^2/(M_A^s)^2)^2}, \qquad F_1^s(q^2) = \mu_s F_2^s(q^2) = 0, \tag{72}$$

with $g_S = -0.15$ and $M_A^s = M_A$.

The vector part in Eq. (71) is conserved, i.e., it is orthogonal to q^μ independently of F_1^s. Because of parity and angular momentum conservation, a pion-in-flight type term can only contribute to the vector part of the matrix element of the $\bar{\Psi}_s \gamma^\mu (1 - \gamma_5)\Psi_s$ operator, and its contribution should be proportional to $(2k_\pi - q)^\mu \bar{u}(\vec{p}\,')\gamma_5 u(\vec{p})$, as in Eq. (51). Assuming a structure of the type $\bar{u}(\vec{p}\,')\gamma_5\gamma^\mu u(\vec{p})$, as in Eq. (51), for the contact term vector contribution to the matrix element of the $\bar{\Psi}_s\gamma^\mu(1 - \gamma_5)\Psi_s$ operator, we will conclude that both types of contributions should be exactly zero to preserve vector current conservation. Within our scheme, we cannot say anything about a possible contact term axial contribution to $\langle p\pi^0|(\bar{\Psi}_s\gamma^\mu(1 - \gamma_5)\Psi_s)(0)|p\rangle$, that for simplicity we will neglect. Thus, we will assume that this latter matrix element is given by the NP and CNP contributions in Eq. (71).

IV. RESULTS

In this section, we will show differential and partially integrated neutrino and antineutrino cross sections for pion production processes driven by both CC and NC. As is usual in pion electroproduction, we will work with angular pion variables $[d\Omega^*(\hat{k}_\pi)]$ defined in the outgoing πN pair CM frame, while the incoming and outgoing lepton variables will be in the LAB frame. We will pay here special attention to the CC pion production cross section dependence on the azimuthal pion angle ϕ_π^* (note that this angle is not affected by the LAB $\rightarrow$ CM boost), and thus we will show the different contributions to $\Sigma^*(q^2, p\cdot q, \theta_\pi^*, \phi_\pi^*)$, defined by its relation to the differential cross section,

$$\frac{d^5\sigma_{\nu_l l}}{d\Omega(\hat{k}')dE'd\Omega^*(\hat{k}_\pi)} = \frac{|\vec{k}'|}{|\vec{k}|}\frac{G^2}{4\pi^2}\Sigma^*, \tag{73}$$

$$\Sigma^*(q^2, p\cdot q, \theta_\pi^*, \phi_\pi^*) = \{A^* + B^*\cos\phi_\pi^* + C^*\cos 2\phi_\pi^* + D^*\sin\phi_\pi^* + E^*\sin 2\phi_\pi^*\}. \tag{74}$$

For the NC case this dependence has been already discussed in Ref. [32] with the aim of distinguishing between ν_τ and $\bar{\nu}_\tau$ below the τ-production threshold, but above the pion production one.

After integrating the pion solid angle, we will take as independent variables the incoming neutrino energy $E = |\vec{k}|$, the invariant mass W of the outgoing pion-nucleon pair $[W^2 = (p + q)^2]$, and the squared of the lepton four-momentum transfer q^2,

$$\frac{d^3\sigma_a}{dq^2dW} = \frac{d^3\sigma_a}{d\Omega(\hat{k}')dE'}\times\frac{\pi W}{ME|\vec{k}'|}, \qquad a = \nu_l l, \nu\nu, \tag{75}$$

where W varies in the range $(m_\pi + M) \le W \le (\sqrt{S} - m_l)$, with $S = (k + p)^2 = M(M + 2E)$. Thus, the incoming neutrino energy in the LAB system, E, should be greater than $m_\pi + m_l + (m_\pi + m_l)^2/2M$ for the pion production process to take place. Besides for a given outgoing πN invariant mass W, q^2 is included in the interval

$$\begin{aligned} q^2_{\rm min}(W) &\equiv [m_l^2 - 2E_{\rm CM}(E'_{\rm CM} + \sqrt{E'^2_{\rm CM} - m_l^2})] \le q^2 \\ &\le [m_l^2 - 2E_{\rm CM}(E'_{\rm CM} - \sqrt{E'^2_{\rm CM} - m_l^2})] \\ &\equiv q^2_{\rm max}(W), \end{aligned} \tag{76}$$

with $E_{\rm CM} = (S - M^2)/2\sqrt{S}$ and $E'_{\rm CM} = (S - W^2 + m_l^2)/2\sqrt{S}$, the incoming neutrino and outgoing lepton energies in the neutrino-nucleon CM frame. It is also useful to perform the phase-space integrals in the other order around, which allows one to find the $d\sigma/dq^2$ differential cross section. The total range of q^2 is given by $q^2_{\rm min}(W = m_\pi + M) \le q^2 \le q^2_{\rm max}(W = m_\pi + M)$, and for a given q^2, the outgoing πN invariant mass W varies:

$$\begin{aligned} W_{\rm min} &\equiv M + m_\pi \le W \\ &\le \left[M^2 + q^2 + 2M\left(\frac{q^2}{q^2 - m_l^2}E - \frac{m_l^2 - q^2}{4E}\right)\right]^{1/2} \\ &\equiv W_{\rm max}(q^2), \end{aligned} \tag{77}$$

where in all equations above, m_l should be set to zero for NC processes.

In the outgoing πN CM frame we will also use that

$$\begin{aligned} \int_0^{+\infty}\frac{d|\vec{k}_\pi||\vec{k}_\pi|^2}{E_\pi}\delta(p'^0 + k_\pi^0 - q^0 - p^0) &= \frac{|\vec{k}_\pi|E'_N}{W}\Big|_{\rm CM} \\ &= \frac{W^2 + M^2 - m_\pi^2}{4W^3}\times\lambda^{1/2}(W^2, M^2, m_\pi^2). \end{aligned} \tag{78}$$

Since the main dynamical ingredients of our model are the excitation of the Δ resonance and the nonresonant contributions deduced from the leading SU(2) nonlinear σ Lagrangian involving pions and nucleons, we will concentrate in the $M + m_\pi \le W \le 1.3$–1.4 GeV region. For larger invariant masses, the chiral expansion will not work, or at least the lowest order used here will not be sufficient [35,36]. Moreover, the effect of heavier resonances will become much more important [19]. Thus, we will limit the available phase-space to guarantee that the invariant mass W will lie in the above range. For a fixed

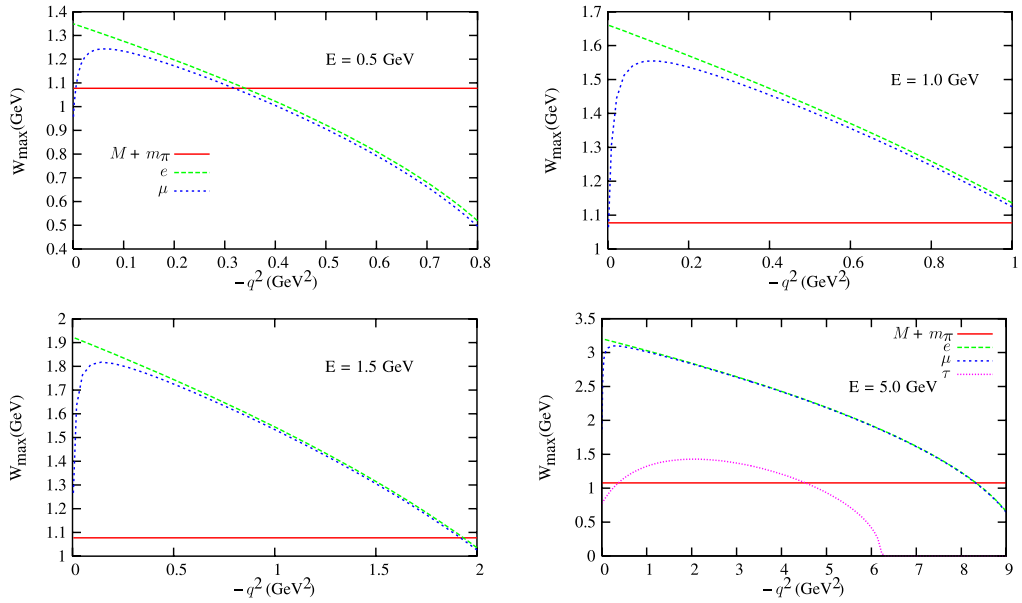

FIG. 3 (color online). Upper integration limit W_{max} as a function of q^2 [Eq. (77)] for incoming neutrino LAB energies $E = 0.5$, 1.0, 1.5, and 5 GeV and different outgoing lepton masses. In all cases the horizontal line stands for the phase-space threshold $M + m_\pi$.

incoming neutrino energy, imposing an upper limit in W will lead to different amounts of phase-space reduction depending on q^2 (see Fig. 3). For neutrino energies of about 1 GeV of relevance in the CC ANL [20] and BNL [21,28] bubble chamber experiments, a great part of the available phase space satisfies the $W \leq 1.3$–1.4 constrain. As the neutrino energy increases, the q^2 interval which leads to CM πN energies around the Δ-resonance pole gets reduced, and the corresponding kinematic cuts performed by the various experiments produce a significant reduction of statistics.

We will see, as also happens in the pion electroproduction case [31], that the inclusion of nonresonant terms (background terms) plays a crucial role close to the $M + m_\pi$ threshold.

A. CC pion production cross sections

There exist several sets of data taken and analyzed in the late seventies and early eighties. The most detailed studies, including measurements, not only of the totally integrated neutrino cross sections, but also of the neutrino flux-averaged q^2 and some angular distributions were made in the ANL 12-foot bubble chamber [20,27] and in the BNL 7-foot deuterium-filled bubble chamber [21,28]. In both experiments the bubble chambers were exposed to a wide band of muon-type neutrino beams with average energies of approximately 1 GeV (ANL) and 1.6 GeV (BNL), and events for the $\nu_\mu p \to \mu^- p \pi^+$, $\nu_\mu n \to \mu^- p \pi^0$, and $\nu_\mu n \to \mu^- n \pi^+$ reactions, with and without a $W \leq 1.4$ GeV cut, were obtained. The ANL experiment used hydrogen and deuterium targets, though most of data come from deuterium exposure. Incoming neutrino energy distributions can be found in Figure 8 of Ref. [37] and in Figure 7 of Ref. [38] for the ANL and BNL experiments, respectively.[13]

Muon-type antineutrino (energy beam peaked around 1.5 GeV) induced total cross sections off the proton (neutron) for final $\pi^- p$ and $\pi^0 n$ ($\pi^- n$) channels with and without the invariant mass cut $W < 1.4$ GeV were measured in the Gargamelle propane experiment at CERN-PS [39].

There also exist experiments at higher neutrino energies carried out at the FNAL 15 ft bubble chamber [40] (neutrino energies from 5 to 100 GeV) and at CERN [41]. In this latter case, a hydrogen target was illuminated with a wide band neutrino and antineutrino beams (energies from 5 to 120 GeV), the mean event energy being about 25 GeV. At such high energies the integrated cross section remains constant with high accuracy, so the exact value of neutrino energy is not important. The implementation of the invariant mass cut $W < 1.4$ GeV reduces significantly the statistics, and we will not consider these data sets in this work.

We start looking at the flux-averaged q^2 differential cross sections for the reaction $\nu_\mu p \to \mu^- p \pi^+$ measured by the ANL and BNL experiments (Fig. 4). In the latter experiment, the cross section overall normalization is not provided. The Δ vector form factors are fixed by electroproduction data, while the axial weak ΔN transition form

[13]Flux-averaged q^2 differential cross sections read

$$\frac{d\overline{\sigma}}{dq^2} = \frac{1}{\mathcal{N}} \int_{E^{min}}^{E^{max}} dE \frac{d\sigma(E)}{dq^2} \Phi(E), \qquad \mathcal{N} = \int_{E^{min}}^{E^{max}} \Phi(E) dE, \tag{79}$$

and similarly for other flux-averaged differential cross sections.

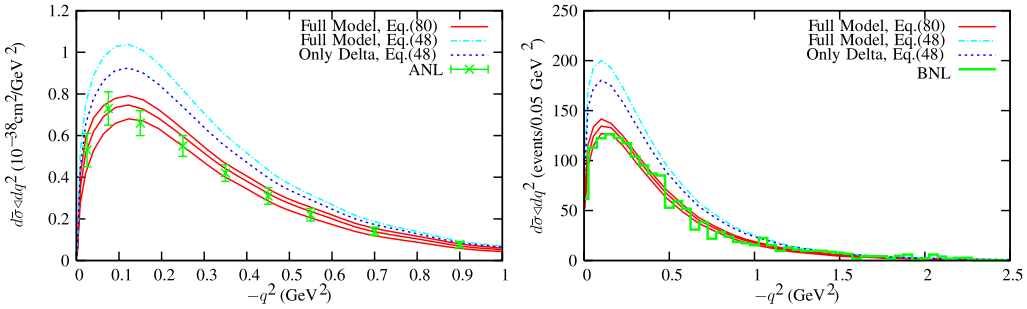

FIG. 4 (color online). Flux-averaged q^2-differential $\nu_\mu p \to \mu^- p \pi^+$ cross section $\int_{M+m_\pi}^{1.4\,\mathrm{GeV}} dW \frac{d\bar{\sigma}_{\nu_\mu \mu^-}}{dq^2 dW}$ compared with the ANL [20] (left) and BNL [21] (right) experiments. Dashed lines stand for the contribution of the excitation of the Δ^{++} resonance and its subsequent decay (ΔP mechanism) with $C_5^A(0) = 1.2$ and $M_{A\Delta} = 1.05$ GeV. Dash-dotted and central solid lines are obtained when the full model of Fig. 2 is considered with $C_5^A(0) = 1.2$, $M_{A\Delta} = 1.05$ GeV (dash-dotted lines) and with our best fit parameters $C_5^A(0) = 0.867$, $M_{A\Delta} = 0.985$ GeV (solid lines). In addition, we also show the 68% CL bands (solid lines) deduced from the Gaussian correlated errors quoted in Eq. (80).

factors have been adjusted in such a way that the Δ^{++} contribution alone would lead to a reasonable description of the shape of the BNL data (see, for instance, Ref. [16]). Moreover, this set of axial form factors also leads to a reasonable description [17] of the ANL data (dashed line in the left panel of Fig. 4). The agreement with the ANL data is certainly worsened when the background terms, required by chiral symmetry, are considered (dash-dotted line). Since the $C_5^A(q^2)$ controls the largest term of the axial contribution, this strongly suggests the readjustment of this form factor. Assuming the same q^2 dependence as in Eq. (48), a χ^2-fit to the flux-averaged ($W < 1.4$ GeV) ANL $\nu_\mu p \to \mu^- p \pi^+$ q^2 differential cross section provides

$$C_5^A(0) = 0.867 \pm 0.075, \qquad M_{A\Delta} = 0.985 \pm 0.082 \text{ GeV}, \tag{80}$$

with a Gaussian correlation coefficient $r = -0.85$ and a $\chi^2/dof = 0.4$. This fitted axial mass in the weak $N\Delta$ vertex is in good agreement with the estimates of about 0.95 GeV and 0.84 GeV given in the original ANL reference [20] and in the work of Ref. [17]. On the other hand, we observe a correction of the order of 30% to the off-diagonal Goldberger-Treiman relation [Eq. (42)]. The lattice QCD results shown in Figure 4 of Ref. [30] might support the ratio $\sqrt{\frac{2}{3}} \frac{f_\pi}{m_\pi} f^*/C_5^A(0)$ becoming significantly larger than unity for realistic pion masses.

The ANL data come mostly from deuterium exposure, and thus deuteron structure effects might affect/are included in this determination of the C_5^A form factor. Such effects were investigated in Ref. [14], where it was estimated that they were always less than 7%. The solid line in the left panel of Fig. 4 shows the quality of the fit. We also plot the 68% confidence level (CL) band deduced from the statistical errors quoted in Eq. (80). We do not fit to the BNL q^2 differential cross section because this data set is given in arbitrary units. To fix the overall BNL data scale, we normalize the area under the theoretical curve, obtained when the full model of Fig. 2 is considered with our best fit parameters $C_5^A(0) = 0.867$, $M_{A\Delta} = 0.985$ GeV, to that under the experimental data. Here again it can be appreciated that, and despite the fact that the isospin factor of the Δ-pole mechanism (with the excitation of the Δ^{++} resonance and its subsequent decay) in this channel is bigger than in the others, the effect of the background terms is quite significant.

Next we show in Fig. 5 the total ANL $\nu_\mu p \to \mu^- p \pi^+$, $\nu_\mu n \to \mu^- p \pi^0$, and $\nu_\mu n \to \mu^- n \pi^+$ cross sections, with the kinematical cut $W < 1.4$ GeV, as a function of the neutrino energy and the predictions of the three schemes defined above: only ΔP contribution with $C_5^A(0) = 1.2$, $M_{A\Delta} = 1.05$ GeV, and the full model derived in this work, including background terms, with the latter set of parameters for $C_5^A(q^2)$ and with that given in Eq. (80). As can be appreciated in the different plots of the figure we achieve a reasonable description of data, finding the largest discrepancies in the $\pi^+ n$ channel. The inclusion of the chiral symmetry background terms derived in this work brings in an overall improved description of the three channels as compared to the case where only the ΔP mechanism is considered. In the case of the $\pi^+ n$ and $\pi^0 p$ cross sections the reduction of the contribution of this latter mechanism is compensated for by the inclusion of the background terms. Our results are similar in quality to those obtained from the model of Ref. [15]. We also display in the various plots of this figure BNL cross section data from Ref. [21] which do not include the $W < 1.4$ GeV cut in the πN invariant mass. For neutrino energies below 1 GeV, the effects of the πN invariant mass cut is almost negligible (see Table III of Ref. [20]). Such effects become much more sizeable for larger neutrino energies (see Table III of Ref. [20]) which have prevented us to present BNL cross section data in the plots for neutrino energies above 1 GeV. We observe some degree of inconsistency among the ANL and BNL measurements. The present

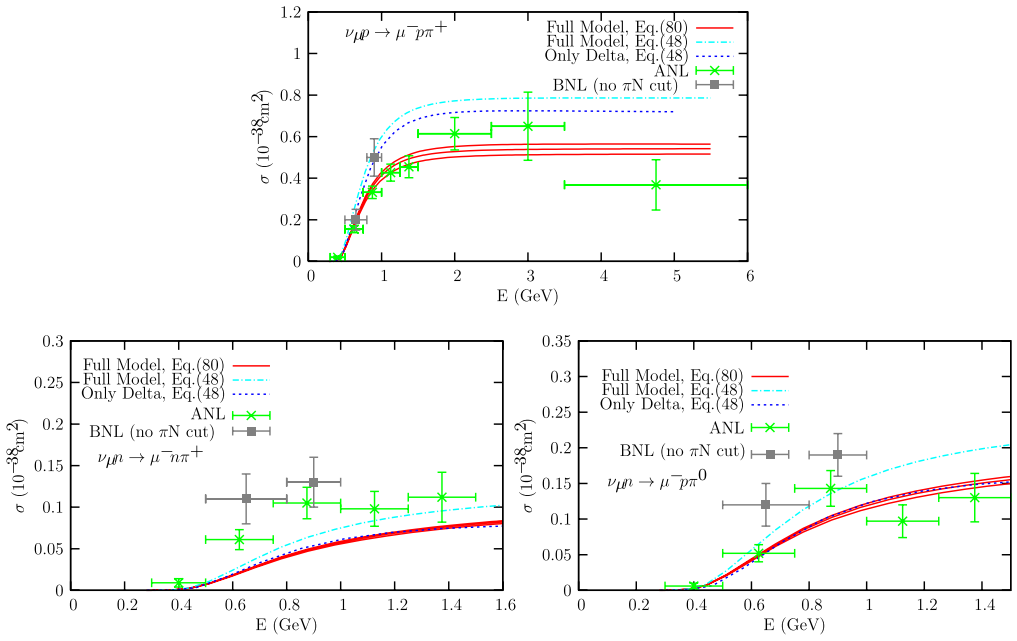

FIG. 5 (color online). Experimental and theoretical results for $\nu_\mu p \to \mu^- p\pi^+$, $\nu_\mu n \to \mu^- p\pi^0$, and $\nu_\mu n \to \mu^- n\pi^+$ cross sections, as a function of the neutrino energy. The ANL results [20] and theoretical cross sections incorporate the kinematical cut $W < 1.4$ GeV. Dashed lines stand for the contribution of the excitation of the Δ resonance and its subsequent decay (ΔP mechanism) with $C_5^A(0) = 1.2$ and $M_{A\Delta} = 1.05$ GeV. Dash-dotted and central solid lines are obtained when the full model of Fig. 2 is considered with $C_5^A(0) = 1.2$, $M_{A\Delta} = 1.05$ GeV (dash-dotted lines) and with our best fit parameters $C_5^A(0) = 0.867$, $M_{A\Delta} = 0.985$ GeV (solid lines). In addition, we also show the 68% CL bands (solid lines) deduced from the Gaussian correlated errors quoted in Eq. (80). We also display BNL cross section data from Ref. [21] which do not include the $W < 1.4$ GeV cut in the πN invariant mass (see text).

model, including nonresonant background terms, with a $C_5^A(q^2)$ form factor consistent with the off-diagonal Goldberger-Treiman relation [Eq. (42)] would lead to a better description of the BNL data (see the dash-dotted lines).

In Fig. 6 we compare the pion azimuthal and pion-nucleon invariant mass distributions (neutrino flux averaged) predicted by the different models examined here with that measured in the ANL experiment [20,26]. For both plots, we normalize the area under the theoretical curve obtained when the full model of Fig. 2 is considered with parameters $C_5^A(0) = 0.867$, $M_{A\Delta} = 0.985$ GeV, to that under the experimental data. The inclusion of chiral background terms leads to a more pronounced ϕ_π^* dependence improving in this way the agreement with the observed event distribution in the ANL experiment. In the right panel of Fig. 6 we show the W-distribution of ANL events, which clearly shows the $\Delta(1232)$ peak. The chiral background terms dominate the distribution near the pion production threshold, and they also produce a slight shift of the maximum of the distribution to lower invariant masses.

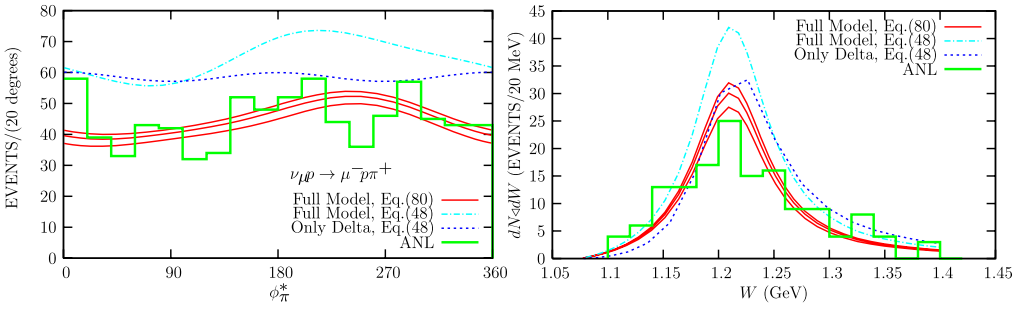

FIG. 6 (color online). Flux-averaged ANL distribution of events in the pion azimuthal angle with $W < 1.4$ GeV (left) and in the πN invariant mass (right) for $\mu^- p\pi^+$ final state. Data taken from Refs. [20,26], respectively. Dashed lines stand for the contribution of the excitation of the Δ^{++} resonance and its subsequent decay (ΔP mechanism) with $C_5^A(0) = 1.2$ and $M_{A\Delta} = 1.05$ GeV. Dash-dotted and central solid lines are obtained when the full model of Fig. 2 is considered with $C_5^A(0) = 1.2$, $M_{A\Delta} = 1.05$ GeV (dash-dotted lines) and with our best fit parameters $C_5^A(0) = 0.867$, $M_{A\Delta} = 0.985$ GeV (solid lines). In addition, we also show the 68% CL bands (solid lines) deduced from the Gaussian correlated errors quoted in Eq. (80).

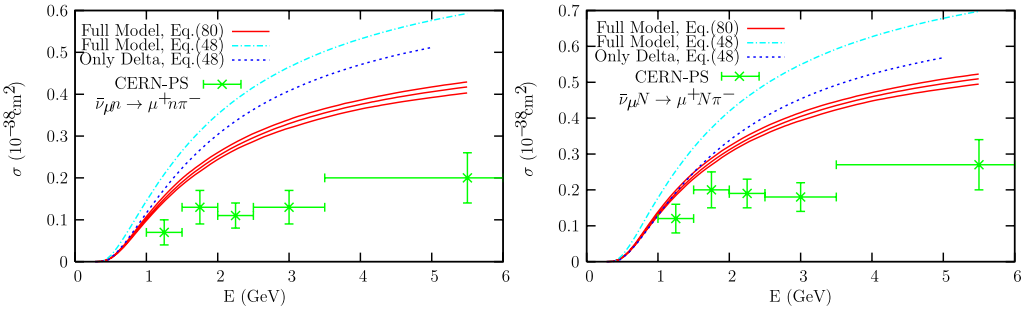

FIG. 7 (color online). Energy dependence of the muon antineutrino cross section, with the invariant mass cut $W \leq 1.4$ GeV, for the $\bar{\nu}_\mu n \to \mu^+ \pi^- n$ (left panel) and the π^- exclusive production (right panel) reactions. Data-points are taken from the CERN-PS experiment of Ref. [39]. Dashed lines stand for the contribution of the excitation of the Δ resonance and its subsequent decay (ΔP mechanism) with $C_5^A(0) = 1.2$ and $M_{A\Delta} = 1.05$ GeV. Dash-dotted and central solid lines are obtained when the full model of Fig. 2 is considered with $C_5^A(0) = 1.2$, $M_{A\Delta} = 1.05$ GeV (dash-dotted lines) and with our best fit parameters $C_5^A(0) = 0.867$, $M_{A\Delta} = 0.985$ GeV (solid lines). In addition, we also show the 68% CL bands (solid lines) deduced from the Gaussian correlated errors quoted in Eq. (80).

In Fig. 7, we compare the predictions of our model with the CERN-PS muon antineutrino cross section data of Ref. [39]. Our model provides larger cross sections than the experiment, but nevertheless, we find here again a reasonable description of the data, which is certainly better than when the ΔP mechanism alone is considered. We would like to remember here that from isospin symmetry we have $\langle n\pi^-|j^\mu_{\mathrm{cc}-}(0)|n\rangle = \langle p\pi^+|j^\mu_{\mathrm{cc}+}(0)|p\rangle$. Therefore, the only dynamical difference between the $\nu_\mu p \to \mu^- p\pi^+$, which we describe correctly (see Fig. 5), and the $\bar{\nu}_\mu n \to \mu^+ p\pi^-$ reactions is the sign of the antisymmetric term of the lepton tensor ($L^{(\bar{\nu})}_{\mu\sigma} = L^{(\nu)}_{\sigma\mu}$). Thus, if one neglects the parity-violating part of the antisymmetric hadronic tensor $(W^{\mu\nu}_{\mathrm{CC}\pi})^{\mathrm{PV}}_a$ [see Eq. (A1) in Appendix A], the cross sections for both reactions will be the same but for differences in the interference between the axial and vector contributions of the hadronic current. However, this vector-axial interference does not affect the sum of the cross sections $\sigma(\nu_\mu p \to \mu^- p\pi^+) + \sigma(\bar{\nu}_\mu n \to \mu^+ p\pi^-)$, except for its contribution to the parity-violating part of the symmetric hadronic tensor. For instance, at $E = 3$ GeV, the experimental value for this sum of cross sections is around 0.78×10^{-38} cm^2, while our best theoretical prediction for it is around 11% bigger. Considering the large errors in experimental data we think this difference is not significant.[14] That might suggest that the discrepancy in the antineutrino cross section might be solved by the inclusion of relative phases between the vector and the axial current theoretical contributions.

Relative signs among the different background contributions are well established, since all of them have been deduced from the same Lagrangian [Eq. (26)] and the vector and axial currents derived from it. One might think in a possible inconsistency between the relative signs of background and resonant pieces. However,

(i) These relative signs are consistent with those deduced from a quark model picture [42].

(ii) As already mentioned, the vector part of the model presented here reduces to that derived in Ref. [31] for the $eN \to e'N\pi$ reaction. Note the relation

$$C_3^V(q^2) = \frac{M}{m_\pi}\sqrt{\frac{2}{3}} f_\gamma(q^2)/e, \tag{81}$$

with $e = \sqrt{4\pi\alpha}$ the proton charge, between C_3^V and the usual $\gamma N\Delta$ coupling, f_γ, used in pion electroproduction reactions (see Eqs. (5) and (A12) in Ref. [31]). This relation is obtained from the nonrelativistic reduction of the C_3^V Dirac structure, which dominates in that limit. Using $f_\gamma(0) \approx 0.122$ as in Ref. [31], one obtains $C_3^V(0) \approx 2.2$, in good agreement with Eq. (46). The model of Ref [31] described[15] reasonably well the available data for the $eN \to e'N\pi$ reaction at low and intermediate energies, including pion angular dependences. This makes us confident on our election of relative signs between resonant and nonresonant terms.

(iii) In what the axial part concerns, we use a consistent sign convention for both the diagonal and off-diagonal Goldberger-Treiman's relations [see the choice of relative signs in Eqs. (27) and (42)].

Nevertheless, in Appendix B we have examined the effect of including relative minus signs between the axial and vector resonant contributions and also between the ΔP and the background terms. Changing the relative sign between the vector and axial contributions of the Δ mechanism is

[14] We note the discrepancy is significantly larger ($\approx 60\%$) if one uses $C_5^A(0) = 1.2$.

[15] A small relative phase between the ΔP and the background terms was also included in Ref. [31]. This phase is deduced from Watson's theorem [43], it depends on q^2 and W, and for the kinematics of interest in this work is comprised in the range 10–20°.

totally discarded by the data, while modifying the relative sign between resonant and nonresonant terms has a little effect, once the W integration is performed. This can be understood by looking at the πN invariant mass distribution of the right panel in Fig. 6. At the Δ peak resonant and nonresonant contributions do not interfere, since the first one is purely imaginary while the latter one is real, and thus in this region the relative sign between both types of contributions is irrelevant. At lower and higher values of W, where the resonant contribution takes also a real part and thus it has a nonvanishing interference with the background terms, there exists a constructive and destructive, respectively, interference. A change of the relative sign between resonant and nonresonant terms would reverse constructive into destructive interferences, and vice-versa, but the net effect after integrating in W is greatly diminished.

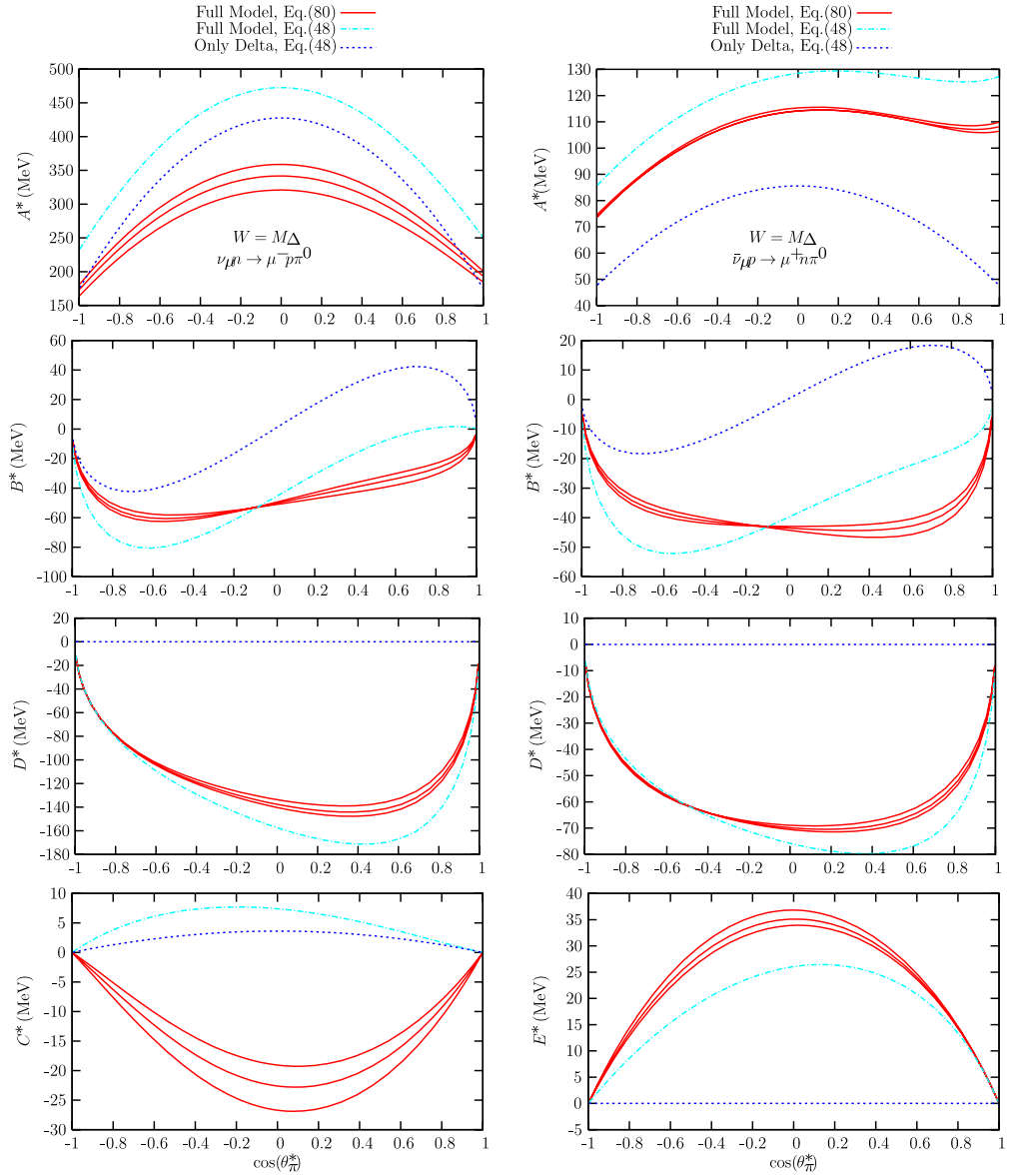

FIG. 8 (color online). Pion polar angle dependence of the ϕ^*_π structure functions defined in Eq. (74) for the $\nu_\mu n \to \mu^- p \pi^0$ and $\bar{\nu}_\mu p \to \mu^+ n \pi^0$ reactions. The neutrino incoming energy is $E = 1.5$ GeV, $q^2 = -0.5$ GeV^2, $W = M_\Delta$ and the pion polar angle is referred to the πN CM frame. Neutrino (antineutrino) A^*, B^*, and D^* structure functions are displayed in the three upper right (left)-hand side plots. The C^* and E^* structure functions, which are equal for both reactions, are shown in the two panels of the last row. Dashed lines stand for the contribution of the excitation of the Δ resonance and its subsequent decay (ΔP mechanism) with $C_5^A(0) = 1.2$ and $M_{A\Delta} = 1.05$ GeV. Dash-dotted and central solid lines are obtained when the full model of Fig. 2 is considered with $C_5^A(0) = 1.2$, $M_{A\Delta} = 1.05$ GeV (dash-dotted lines) and with our best fit parameters $C_5^A(0) = 0.867$, $M_{A\Delta} = 0.985$ GeV (solid lines). In addition, we also show the 68% CL bands (solid lines) deduced from the Gaussian correlated errors quoted in Eq. (80).

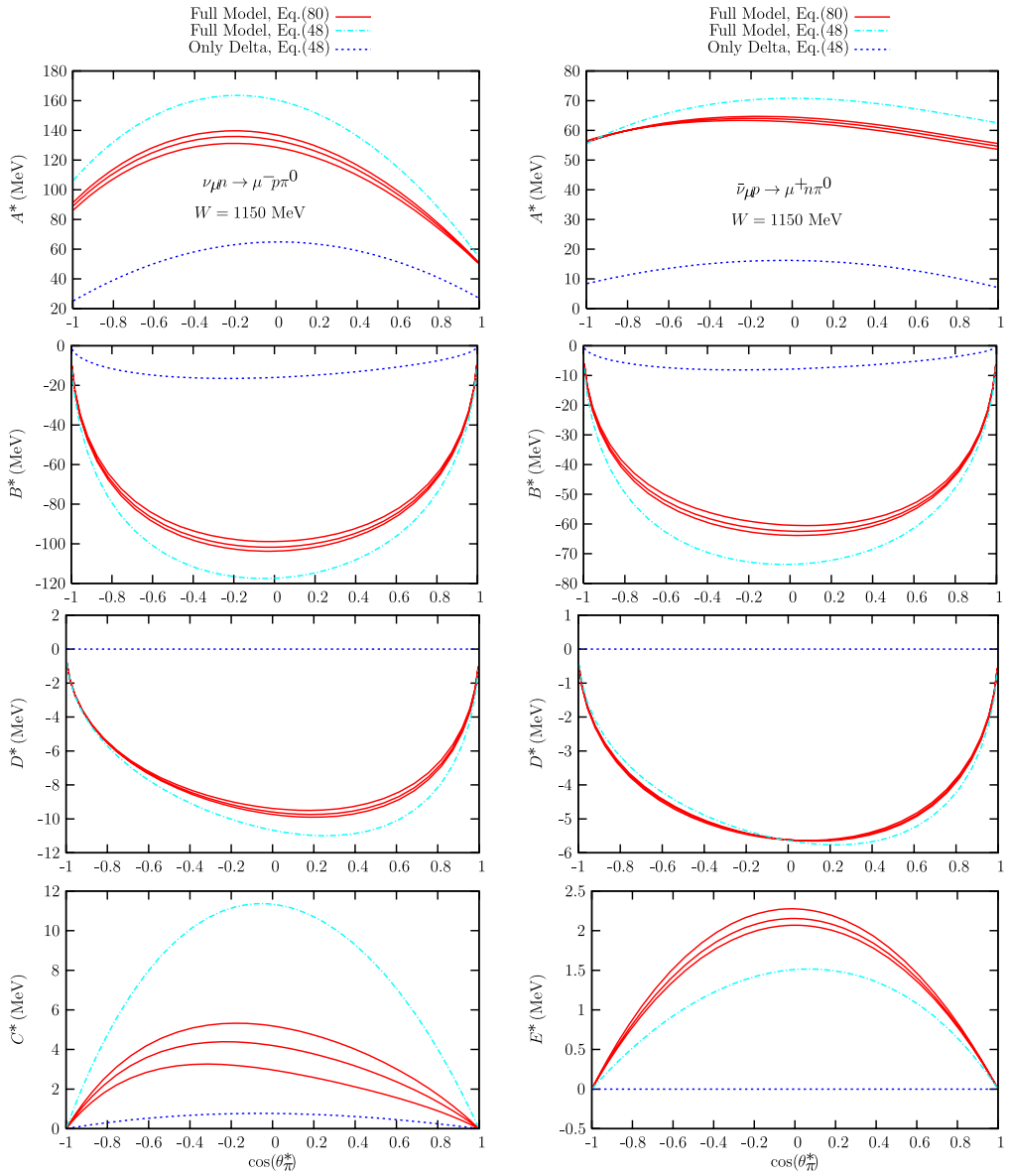

FIG. 9 (color online). Same as in Fig. 8 for $W = 1150$ MeV.

After this discussion, we stress that one would need relative phases (and not merely minus signs) between vector and axial resonant and nonresonant contributions to improve the combined description of neutrino and antineutrino cross sections. However, very recently S. K. Singh and collaborators have pointed out [44] that nuclear medium effects and pion absorption (note that the antineutrino data of Ref. [39] presented in Fig. 7 were measured on Freon-propane) were not properly taken into account in the original work of Bolognese and collaborators [39]. In this manner, the apparent discrepancies highlighted by the former discussion might disappear (see Figs. 17 and 18 of Ref. [44]). More accurate data, possibly available in the future from the MiniBoone and T2K experiments, in conjunction with Watson's theorem [43] might shed light into this interesting issue.

Next we pay attention to the differential cross section decomposition of Eq. (74) following the different allowed dependences on the pion azimuthal angle. In Figs. 8 and 9 we simultaneously compare results for the $\nu_\mu n \to \mu^- p\pi^0$ and $\bar{\nu}_\mu p \to \mu^+ n\pi^0$ reactions. Thanks to isospin symmetry [see Eq. (13)], the hadronic tensor is the same for both processes and hence, they are only distinguished by the different neutrino- and antineutrino-induced lepton vertices, which produces a change of sign in the antisymmetric part of the leptonic tensor. Therefore, and following Eqs. (A8) and (A9), the C^* and E^* structure functions are equal for both reactions, while the antisymmetric contributions to the neutrino and antineutrino A^*, B^*, and D^* ones change sign. We fix $E = 1.5$ GeV and $q^2 = -0.5$ GeV^2, which naturally lies into the ANL kinematics,

TABLE I. NC to CC ($\nu p \to \mu^- p \pi^+$) cross section ratios. Experimental data taken from the ANL analyses of Refs. [48] (R_-) and [49] (R_0, R_+). Our results are obtained for an incoming neutrino energy range of $E = 0.6$–1.2 GeV using our full model of Fig. 2 and with our best fit parameters $C_5^A(0) = 0.867$, $M_{A\Delta} = 0.985$ GeV. No kinematical cut in the W invariant mass has been used.

	ANL	Our results
$R_+ = \sigma(\nu p \to \nu n \pi^+)/\sigma(\nu p \to \mu^- p \pi^+)$	0.12 ± 0.04 [49]	0.12 − 0.10
$R_0 = \sigma(\nu p \to \nu p \pi^0)/\sigma(\nu p \to \mu^- p \pi^+)$	0.09 ± 0.05 [49]	0.18 − 0.14
$R_- = \sigma(\nu n \to \nu p \pi^-)/\sigma(\nu p \to \mu^- p \pi^+)$	0.11 ± 0.022 [48]	0.12 − 0.09

and we consider two different πN invariant masses, $W = 1150$ MeV and $W = M_\Delta$, to better understand the effect of the chiral symmetry background terms on the structure functions defined in Eq. (74). Results displayed in these plots show clearly both the difference between neutrino and antineutrino structure functions and the effect of the chiral symmetry background terms on them. For instance in the $W = M_\Delta$ case, neutrino and antineutrino A^* structure functions differ by about a factor of 3, which will provide a similar factor in the integrated cross sections. In these channels, background terms have a greater influence in the antineutrino-induced process than in the neutrino one. On the other hand, for $W = 1150$ MeV the ΔP mechanism becomes subdominant and the bulk of the structure functions is determined by the background terms and their interferences with the ΔP one.

Besides, the interference between the ΔP mechanism and the rest of the chiral background terms leads to nonvanishing D^* and E^* structure functions. These functions provide dependences in $\sin\phi_\pi^*$ and $\sin 2\phi_\pi^*$ and arise from the parity-violating terms in the hadronic tensor decomposition in Eq. (A1). These parity-violating contributions to the fifth differential cross section $d^5\sigma_{\nu_l}/d\Omega(\hat{k}')dE'd\Omega(\hat{k}_\pi)$ disappear when the pion solid angle integration is performed, as required by the scalar, up to the factor $|\vec{k}'|/|\vec{k}|$, nature of the triple differential cross section $d^3\sigma_{\nu_l}/d\Omega(\hat{k}')dE'$. Note that the coordinate system used to define $d\Omega(\hat{k}_\pi)$ involves the pseudovector $\vec{k} \times \vec{k}'$ to set up the Y-axis, which induces the nonparity invariant nature of $d^5\sigma/d\Omega(\hat{k}')dE'd\Omega(\hat{k}_\pi)$. In electropion production processes, the leptonic tensor is purely symmetric, and the symmetric part of the hadronic one cannot contain terms involving the Levi-Cività tensor, since the electromagnetic interaction preserves parity. Hence, in that case $d^5\sigma/d\Omega(\hat{k}')dE'd\Omega(\hat{k}_\pi)$ turns out to be a scalar under parity. Moreover, these terms also induce T-odd correlations in the $(L^{(\nu,\bar{\nu})})_{\mu\nu}W^{\mu\nu}$ contraction [see Eqs. (A1)–(A7) in the Appendix A], which do not imply a genuine violation of time-reversal invariance because of the existence of strong final state interaction effects[16] [45,46].

[16]Within our formalism, the inclusion of the Δ resonance width accounts partially for the strong final state effects.

B. NC pion production cross sections

There hardly exist [47–49] NC experimental measurements at intermediate energies. In the Gargamelle propane-Freon experiment run at CERN [47], the NC neutrino-induced pion production cross sections, in all possible channels, were measured at averaged neutrino energy of around 2.2 GeV, and given in the form of NC/CC ratios. These data have been reanalyzed, and absolute cross sections, without imposing any cut in the pion-nucleon invariant mass, have been recently provided [50]. Experiments using the Argonne 12-ft deuterium bubble chamber were run over a neutrino energy interval ($0.3 \leq E \leq 1.5$) GeV [48,49]. These latter experiments gave results for the NC $\nu n \to \nu p \pi^-$ cross section [48], as well as the NC to CC cross section ratios $R_+ = \sigma(\nu p \to \nu n \pi^+)/\sigma(\nu p \to \mu^- p \pi^+)$, $R_0 = \sigma(\nu p \to \nu p \pi^0)/\sigma(\nu p \to \mu^- p \pi^+)$ [49], and $R_- = \sigma(\nu n \to \nu p \pi^-)/\sigma(\nu p \to \mu^- p \pi^+)$ [48].

The NC pion production reaction was proposed in Ref. [32] as a potential tool to distinguish τ-neutrinos from antineutrinos, below the τ-production threshold, but above the pion production one. Model independent neutrino-antineutrino asymmetries both in the totally integrated cross sections and in the pion azimuthal differential distributions were predicted in Ref. [32]. Results of the current model for these neutrino-antineutrino asymmetries were presented there. Here, we will focus on the comparison of our results with the available experimental data as well as emphasizing other aspects of the NC pion production processes.

In Table I we compare our results for the R_+, R_0, and R_- NC over CC ratios with the ANL experimental data. Our results are obtained for an incoming neutrino energy range of $E = 0.6$–1.2 GeV using our full model of Fig. 2 and with our best fit parameters $C_5^A(0) = 0.867$, $M_{A\Delta} = 0.985$ GeV. We find a fair agreement for all ratios, when the experimental uncertainties are taken into account.

In Table II we present results for the total NC cross sections in different channels at $E = 2.2$ GeV and compare them with the reanalysis done in Ref. [50] of the original data by the Gargamelle experiment at CERN [47]. We use our full model of Fig. 2 with our best fit parameters $C_5^A(0) = 0.867$, $M_{A\Delta} = 0.985$ GeV with no upper limit in the W-integration to allow a direct comparison with the experiment. The agreement with data is good.

TABLE II. NC cross sections in units of 10^{-38} cm^2 for different channels. Data shown correspond to the results of a recent reanalysis [50] of the original data taken by the Gargamelle experiment at CERN [47]. Our results are obtained for an incoming neutrino energy of $E = 2.2$ GeV using our full model of Fig. 2 and with our best fit parameters $C_5^A(0) = 0.867 \pm 0.075$, $M_{A\Delta} = 0.985 \pm 0.082$ GeV. No cut in the pion-nucleon invariant mass W has been applied and we Monte Carlo propagate the latter errors to our results for the cross sections.

	[50]	Our results
$\sigma(\nu p \to \nu p \pi^0)$	0.130 ± 0.020	0.105 ± 0.006
$\sigma(\nu p \to \nu n \pi^+)$	0.080 ± 0.020	0.091 ± 0.003
$\sigma(\nu n \to \nu n \pi^0)$	0.080 ± 0.020	0.104 ± 0.006
$\sigma(\nu n \to \nu p \pi^-)$	0.110 ± 0.030	0.082 ± 0.003

However a word of caution is in order here. As we discussed above, our model suffers from larger uncertainties in the $W > 1.4$ GeV region which will be accessible for neutrinos of this energy.

In the left panel of Fig. 10 we show our results for the $\nu n \to \nu p \pi^-$ cross section as a function of the energy and compare them with the ANL data of Ref. [48]. There, and to better compare with the data, we also give results without the $W \leq 1.4$ GeV constraint. Up to incoming neutrino LAB energies of the order of 1 GeV the implementation of this cut hardly changes the cross section. We find a good description of the data. In the right panel of Fig. 10 we show the W-differential cross section for the same channel and neutrinos of 1 GeV. There one can appreciate clearly the $\Delta(1232)$ peak. The chiral background terms dominate the differential cross section near the pion production threshold, and they also produce a slight shift of the maximum of the cross section to lower invariant masses, as also happened in the distribution of CC events displayed in Fig. 6. In both plots we see that the reduction of the contribution of the ΔP mechanism, due to the diminution of the value of $C_5^A(0)$, is partially compensated by the inclusion of the background terms.

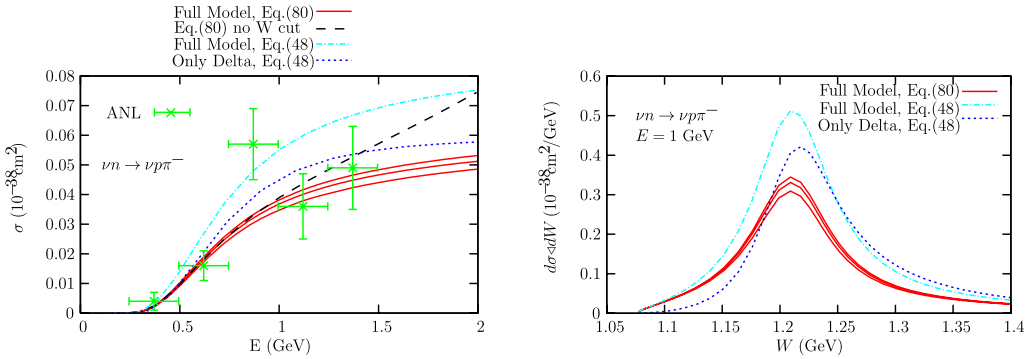

FIG. 10 (color online). Total (left) and W-differential (right) cross sections for the $\nu n \to \nu p \pi^-$ reaction. Left panel data are taken from Ref. [48] and have been measured without limiting the pion–nucleon invariant mass W. Dashed lines stand for the contribution of the excitation of the Δ resonance and its subsequent decay (ΔP mechanism) with $C_5^A(0) = 1.2$ and $M_{A\Delta} = 1.05$ GeV. Dash-dotted and central solid lines are obtained when the full model of Fig. 2 is considered with $C_5^A(0) = 1.2$, $M_{A\Delta} = 1.05$ GeV (dash-dotted lines) and with our best fit parameters $C_5^A(0) = 0.867$, $M_{A\Delta} = 0.985$ GeV (solid lines). In addition, we also show the 68% CL bands (solid lines) deduced from the Gaussian correlated errors quoted in Eq. (80). In all these cases, we have limited the invariant mass phase-space ($W \leq 1.4$ GeV). In the left-hand side panel the long-dashed line stands for our full model results without including the $W \leq 1.4$ GeV cut. The LAB incoming neutrino energy in the right-hand side plot is 1 GeV.

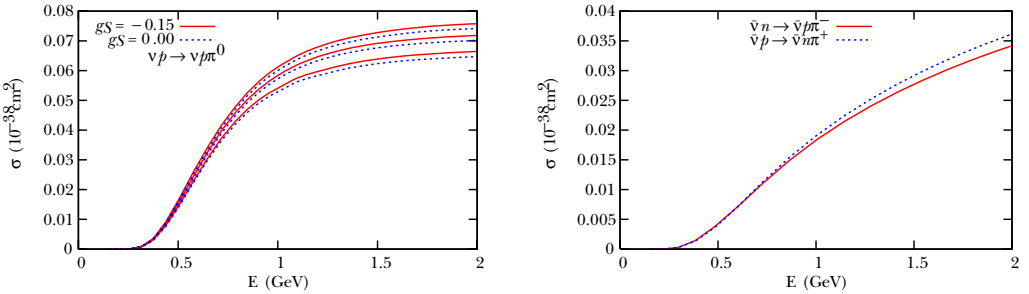

FIG. 11 (color online). Total $\nu p \to \nu p \pi^0$ (left panel), $\bar{\nu} n \to \bar{\nu} p \pi^-$, and $\bar{\nu} p \to \bar{\nu} n \pi^+$ (right panel) cross sections, with the $W \leq 1.4$ GeV cut, as a function of the neutrino or antineutrino energy. In the left panel we show results obtained for two different values of the nucleon strange content [g_S in Eq. (72)] with the full model of Fig. 2 and our fitted $C_5^A(q^2)$ form factor. We also include the 68% CL bands inferred from Eq. (80). In the right panel we do not give the CL bands and g_S is set to -0.15.

Next, we study the effect of the strange content of the nucleon within our model (left panel of Fig. 11). We find that effects are even smaller than the statistical uncertainties deduced from the fit of the $C_5^A(q^2)$ form factor to the ANL data in Eq. (80). Similarly, results of the right panel of this figure show that the isovector part of the NC completely dominates the pion production reaction at the intermediate energies studied here. This is because, as can be deduced from Eqs. (64), (65), and (70), both cross sections just differ in the interference between the isovector and the isoscalar parts of the NC. Finally, we would like to mention that antineutrino-induced cross sections are around a factor 2 or 3 smaller than neutrino-induced ones, as can be appreciated by comparing predictions for the $p\pi^-$ final state given in the left panel of Fig. 10 and the right panel of Fig. 11.

V. CONCLUSIONS

We have developed a model for the weak pion production off the nucleon driven both by CC and NC at intermediate energies, which improves most of the existing ones. Besides the ΔP mechanism, we have also included some background terms, required by chiral symmetry. Starting from an SU(2) nonlinear σ model involving pions and nucleons, which implements the pattern of spontaneous chiral symmetry breaking of QCD, we derive the corresponding vector and axial currents [up to order $\mathcal{O}(1/f_\pi^3)$] which determine the structure of the chiral nonresonant terms. Vector current conservation and PCAC are also employed to establish some relations between the weak form factors. In this way constructed, this model represents the natural extension of that developed in Ref. [31] for the $eN \to e'N'\pi$ reaction.

As a result of the inclusion of the background contributions, we had to refit the $C_5^A(q^2)$ form factor to the flux-averaged $\nu_\mu p \to \mu^- p\pi^+$ ANL q^2-differential cross section data with $W < 1.4$, finding a smaller contribution of the ΔP mechanism than traditionally assumed in the literature [see Eq. (80)]. We find a correction of the order of 30% to the off-diagonal Goldberger-Treiman relation [Eq. (42)], which we interpret is not in conflict with the lattice QCD results shown in Figure 4 of Ref. [30], if they were extrapolated to realistic pion masses. Within this scheme, we have calculated several differential and integrated[17] cross sections, including pion angular distributions, induced by neutrinos and antineutrinos and driven both by CC and NC. In all cases we find that the background terms produce quite significant effects, and for those quantities where there are experimental measurements, we find that the inclusion of these terms brings in an overall improved description of the data, as compared to the case where only the ΔP mechanism is considered. We give 68% CL bands for most of the computed observables as deduced from the Gaussian correlated errors quoted in Eq. (80). For NC reactions the isoscalar contribution is quite small and, in particular, we find the nucleon strange content effects are smaller than the statistical uncertainties deduced from the fit of $C_5^A(q^2)$ to the ANL data.

At higher πN invariant masses than those considered in this work, heavier resonances than the $\Delta(1232)$ [as for example $N(1440), N(1535), N(1520), \ldots$] will certainly play an important role. However, we might safely expect the contribution of these heavier resonances to be negligible at pion threshold, where the chiral background terms computed in this work are dominant, and that it would remain quite small up to the πN invariant masses around 1.3–1.4 GeV considered here [19].

We also show that the interference between the ΔP and the background terms produces parity-violating contributions to the fifth differential cross section $d^5\sigma_{\nu_l l}/d\Omega(\hat{k}')dE'd\Omega(\hat{k}_\pi)$, which are intimately linked to T-odd correlations in the $(L^{(\nu,\bar{\nu})})_{\mu\nu}W^{\mu\nu}$ contraction. However, these latter correlations do not imply a genuine violation of time-reversal invariance because of the existence of strong final state interaction effects.

The extension of this work to the study of the weak two-pion production off the nucleon near threshold is natural and will be presented elsewhere [51].

ACKNOWLEDGMENTS

We thank M. J. Vicente-Vacas and L. Alvarez-Ruso for useful discussions. This work was supported by DGI and FEDER funds, under Contracts No. FIS2005-00810, No. BFM2003-00856, No. FPA2004-05616, and No. FIS2006-03438, by Junta de Andalucía and Junta de Castilla y León under Contracts No. FQM0225, No. SA104/04, No. SA016A07, and it is a part of the EU Integrated Infrastructure Initiative Hadron Physics Project Contract No. RII3-CT-2004-506078.

APPENDIX A: DEPENDENCE OF THE NEUTRINO DIFFERENTIAL CROSS SECTION ON THE OUTGOING PION AZIMUTHAL ANGLE

The hadronic tensor is completely determined by up to a total of 19 Lorentz scalar and real, structure functions [32] $W_i(q^2, p\cdot q, p\cdot k_\pi, k_\pi\cdot q)$,

$$(W^{\mu\nu}_{\mathrm{CC}\pi})^{(\nu)}_{s,a} = (W^{\mu\nu}_{\mathrm{CC}\pi})^{(\nu),\mathrm{PC}}_{s,a} + (W^{\mu\nu}_{\mathrm{CC}\pi})^{(\nu),\mathrm{PV}}_{s,a}, \qquad \text{(A1)}$$

where the labels PC and PV stand for parity-conserving and parity-violating contributions, and (for simplicity from now on we drop the CCπ and (ν) labels in the notation of the hadronic tensor)

[17]There are some inconsistencies among the ANL and BNL totally integrated cross section data (Fig. 5), and we would obtain a better description of the BNL data with a $C_5^A(q^2)$ form factor consistent with the off-diagonal Goldberger-Treiman relation.

$$(W^{\mu\nu})_s^{\rm PC} = W_1 g^{\mu\nu} + W_2 p^\mu p^\nu + W_3 q^\mu q^\nu + W_4 k_\pi^\mu k_\pi^\nu + W_5(q^\mu p^\nu + q^\nu p^\mu) + W_6(q^\mu k_\pi^\nu + q^\nu k_\pi^\mu) + W_7(p^\mu k_\pi^\nu + p^\nu k_\pi^\mu), \quad \text{(A2)}$$

$$(W^{\mu\nu})_s^{\rm PV} = W_8(q^\mu \epsilon^\nu_{.\alpha\beta\gamma} k_\pi^\alpha p^\beta q^\gamma + q^\nu \epsilon^\mu_{.\alpha\beta\gamma} k_\pi^\alpha p^\beta q^\gamma) + W_9(p^\mu \epsilon^\nu_{.\alpha\beta\gamma} k_\pi^\alpha p^\beta q^\gamma + p^\nu \epsilon^\mu_{.\alpha\beta\gamma} k_\pi^\alpha p^\beta q^\gamma) + W_{10}(k_\pi^\mu \epsilon^\nu_{.\alpha\beta\gamma} k_\pi^\alpha p^\beta q^\gamma + k_\pi^\nu \epsilon^\mu_{.\alpha\beta\gamma} k_\pi^\alpha p^\beta q^\gamma), \quad \text{(A3)}$$

$$(W^{\mu\nu})_a^{\rm PV} = W_{11}(q^\mu p^\nu - q^\nu p^\mu) + W_{12}(q^\mu k_\pi^\nu - q^\nu k_\pi^\mu) + W_{13}(p^\mu k_\pi^\nu - p^\nu k_\pi^\mu), \quad \text{(A4)}$$

$$(W^{\mu\nu})_a^{\rm PC} = W_{14}\epsilon^{\mu\nu\alpha\beta} p_\alpha q_\beta + W_{15}\epsilon^{\mu\nu\alpha\beta} p_\alpha k_{\pi\beta} + W_{16}\epsilon^{\mu\nu\alpha\beta} q_\alpha k_{\pi\beta} + W_{17}(q^\mu \epsilon^\nu_{.\alpha\beta\gamma} k_\pi^\alpha p^\beta q^\gamma - q^\nu \epsilon^\mu_{.\alpha\beta\gamma} k_\pi^\alpha p^\beta q^\gamma) + W_{18}(p^\mu \epsilon^\nu_{.\alpha\beta\gamma} k_\pi^\alpha p^\beta q^\gamma - p^\nu \epsilon^\mu_{.\alpha\beta\gamma} k_\pi^\alpha p^\beta q^\gamma) + W_{19}(k_\pi^\mu \epsilon^\nu_{.\alpha\beta\gamma} k_\pi^\alpha p^\beta q^\gamma - k_\pi^\nu \epsilon^\mu_{.\alpha\beta\gamma} k_\pi^\alpha p^\beta q^\gamma). \quad \text{(A5)}$$

The tensor $(W^{\mu\nu})^{\rm PV} = (W^{\mu\nu})_s^{\rm PV} + {\rm i}(W^{\mu\nu})_a^{\rm PV}$ when contracted with the leptonic one, $L_{\mu\nu}^{(\nu)}$, provides a pseudoscalar quantity; i.e., such contraction is not invariant under a parity transformation. Indeed, under a parity transformation we have

$$L_{\mu\nu}^{(\nu)} \to (L^{\nu\mu})^{(\nu)}, \qquad (W_{\mu\nu})^{\rm PV} \to -(W^{\nu\mu})^{\rm PV}, \quad \text{(A6)}$$

whereas the tensor $(W^{\mu\nu})^{\rm PC} = (W^{\mu\nu})_s^{\rm PC} + {\rm i}(W^{\mu\nu})_a^{\rm PC}$ transforms as $(L^{\mu\nu})^{(\nu)}$. This explains the origin of the adopted labels PC and PV. The triple differential cross section $d^3\sigma_{\nu_l l}/d\Omega(\hat{k}')dE'$ is a scalar, up to the factor $|\vec{k}'|/|\vec{k}|$. Thus all parity-violating contributions must disappear when performing the pion solid angle integration. A further remark concerns the time-reversal (T) violation effects apparently encoded in the decomposition of the hadronic tensor in Eqs. (A1)–(A5). Under a time-reversal transformation, and taking into account the antiunitary character of the T-operator, we have

$$L_{\mu\nu}^{(\nu)} \to (L^{\mu\nu})^{(\nu)}, \qquad (W_{\mu\nu})_{\rm PC} \to (W^{\mu\nu})^{\rm PC}, \qquad (W_{\mu\nu})^{\rm PV} \to -(W^{\mu\nu})^{\rm PV}, \quad \text{(A7)}$$

and therefore $(L^{(\nu)})_{\mu\nu} W^{\mu\nu}$ is not T-invariant either, because of the presence of the PV terms in the hadronic tensor.[18] This does not necessarily mean that there exists a violation of T-invariance in the process because of the existence of strong final state interaction effects [45,46].

With our election of kinematics ($\vec{k}$, $\vec{k}'$ in the XZ-plane), we find $(L_s^{(\nu)})_{0y} = (L_s^{(\nu)})_{xy} = (L_s^{(\nu)})_{zy} = (L_a^{(\nu)})_{0x} = (L_a^{(\nu)})_{0z} = (L_a^{(\nu)})_{xz} = 0$, and then

$$\int_0^{+\infty} \frac{dk_\pi k_\pi^2}{E_\pi} (L_s^{(\nu)})_{\mu\nu} W_s^{\mu\nu} = \int_0^{+\infty} \frac{dk_\pi k_\pi^2}{E_\pi} \{(L_s^{(\nu)})_{00} W_s^{00} + 2(L_s^{(\nu)})_{0x} W_s^{0x} + 2(L_s^{(\nu)})_{0z} W_s^{0z} + (L_s^{(\nu)})_{xx} W_s^{xx} + (L_s^{(\nu)})_{yy} W_s^{yy} + (L_s^{(\nu)})_{zz} W_s^{zz} + 2(L_s^{(\nu)})_{xz} W_s^{xz}\}$$
$$= A_s + B_s \cos\phi_\pi + C_s \cos 2\phi_\pi + D_s \sin\phi_\pi + E_s \sin 2\phi_\pi, \quad \text{(A8)}$$

$$\int_0^{+\infty} \frac{dk_\pi k_\pi^2}{E_\pi} (L_a^{(\nu)})_{\mu\nu} W_a^{\mu\nu} = 2\int_0^{+\infty} \frac{dk_\pi k_\pi^2}{E_\pi} \{(L_a^{(\nu)})_{0y} W_a^{0y} + (L_a^{(\nu)})_{xy} W_a^{xy} + (L_a^{(\nu)})_{yz} W_a^{yz}\} = -A_a - B_a \cos\phi_\pi - D_a \sin\phi_\pi, \quad \text{(A9)}$$

where we explicitly show the ϕ_π dependence.[19] The PV term of the hadronic tensor has led to the parity-violating $\sin\phi_\pi$ and $\sin 2\phi_\pi$ contributions (all of them proportional to $k_{\pi y}$). They disappear when the pion solid angle integration is performed, as anticipated. The above equations automatically imply Eq. (7).

[18] Note that transformations given in Eqs. (8), (A6), and (A7) imply that the leptonic tensor, by itself, is invariant under CPT.

[19] All structure functions, $W_{i=1,\ldots,19}$, depend on the Lorentz scalar $p\cdot k_\pi$ and $k_\pi \cdot q$ factors, which are functions of the angle formed between the $\vec{q}$ and $\vec{k}_\pi$ vectors, and thus they are independent of ϕ_π, when $\vec{q}$ is taken along the Z-axis.

APPENDIX B: VECTOR-AXIAL RESONANT AND RESONANT-NONRESONANT RELATIVE SIGNS

Because of the poor description of the muon antineutrino cross section data of Ref. [39] (see Fig. 7) achieved with the different models studied in this work, we examined here the effect of including relative minus signs between the axial and vector resonant contributions and also between the ΔP and the background terms. We have focused on the flux-averaged $\nu_\mu p \to \mu^- p\pi^+$ ANL q^2-differential cross section displayed in the left panel of Fig. 4, and on the total $\nu_\mu p \to \mu^- p\pi^+$ and $\bar{\nu}_\mu n \to \mu^+ p\pi^-$ cross sections given as a function of the neutrino/antineutrino energy in the top and left panels of

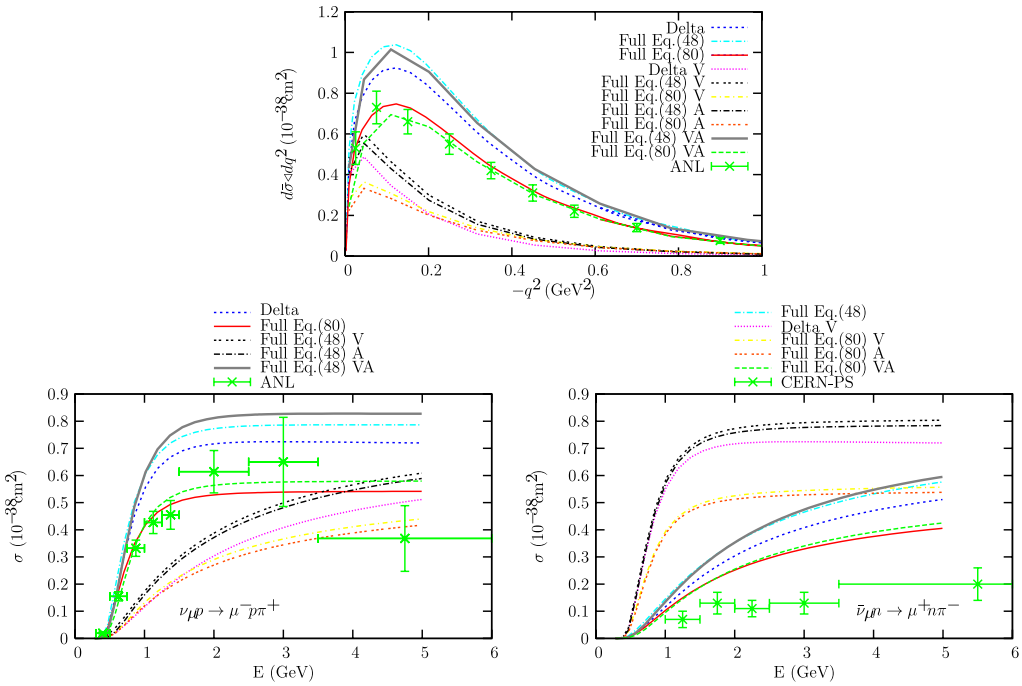

FIG. 12 (color online). Flux-averaged $\nu_\mu p \to \mu^- p \pi^+$ ANL q^2-differential cross section (top) and total $\nu_\mu p \to \mu^- p \pi^+$ and $\bar{\nu}_\mu n \to \mu^+ p \pi^-$ cross sections as a function of the neutrino/antineutrino energy (bottom) from different choices of the vector-axial resonant and resonant-nonresonant relative signs (see text for details).

Figs. 5 and 7, respectively. Results of our analysis are presented in Fig. 12. There, and in addition to the results obtained from the three models presented up to now [excitation of the Δ resonance and its subsequent decay, ΔP mechanism, with $C_5^A(0) = 1.2$ and $M_{A\Delta} = 1.05$ GeV (dashed lines), and the full model of Fig. 2 with $C_5^A(0) = 1.2$, $M_{A\Delta} = 1.05$ GeV (dash-dotted lines), and with our best fit parameters $C_5^A(0) = 0.867$, $M_{A\Delta} = 0.985$ GeV (solid lines)] with the set of signs deduced in our scheme, we also show results from different choices of the relative signs. Curves denoted by V(A) have been obtained by changing the sign of the $WN\Delta$ vector (axial) form factors in Eq. (40), and similarly results denoted by VA have been obtained by including an extra minus sign between the ΔP and the background contributions. Changing the sign of either the vector or the axial contributions of the Δ mechanism is strongly disfavored by the data, while modifying the relative sign between resonant and nonresonant terms has a little effect, as we already mentioned in the discussion of Fig. 7.

These results provide a further confirmation of the sign convention used in this work, and the muon antineutrino discrepancies of Fig. 7 point out to the existence of nontrivial relative phases (and not merely minus signs) between vector and axial resonant and nonresonant contributions and/or more likely that some nuclear medium effects were not properly discounted [44] in Ref. [39], when providing cross sections off the nucleon from measurements obtained in the liquid bubble chamber Gargamelle that was filled with propane and a small admixture of heavy Freon CF_3Br.

[1] M. Honda, T. Kajita, K. Kasahara, and S. Midorikawa, Phys. Rev. D **52**, 4985 (1995).
[2] F. Vissani and A. Yu. Smirnov, Phys. Lett. B **432**, 376 (1998).
[3] S. Nakayama *et al.*, Phys. Lett. B **619**, 255 (2005).
[4] J. L. Raaf, Nucl. Phys. B, Proc. Suppl. **139**, 47 (2005).
[5] J. Nieves, J. E. Amaro, and M. Valverde, Phys. Rev. C **70**, 055503 (2004); **72**, 019902(E) (2005).
[6] M. Valverde, J. E. Amaro, and J. Nieves, Phys. Lett. B **638**, 325 (2006).
[7] J. Nieves, M. Valverde, and M. J. Vicente Vacas, Phys. Rev. C **73**, 025504 (2006).
[8] S. L. Adler, Ann. Phys. (N.Y.) **50**, 189 (1968).
[9] C. H. Llewellyn Smith, Phys. Rep. **3C**, 261 (1972).
[10] P. A. Schreiner and F. von Hippel, Phys. Rev. Lett. **30**, 339 (1973).

[11] G. L. Fogli and G. Nardulli, Nucl. Phys. **B160**, 116 (1979).
[12] G. L. Fogli and G. Nardulli,Nucl. Phys. **B165**, 162 (1980).
[13] L. Alvarez-Ruso, S. K. Singh, and M. J. Vicente Vacas, Phys. Rev. C **57**, 2693 (1998).
[14] L. Alvarez-Ruso, S. K. Singh, and M. J. Vicente Vacas, Phys. Rev. C **59**, 3386 (1999).
[15] T. Sato, D. Uno, and T. S. H. Lee, Phys. Rev. C **67**, 065201 (2003).
[16] E. A. Paschos, J.-Y. Yu, and M. Sakuda, Phys. Rev. D **69**, 014013 (2004).
[17] O. Lalakulich and E. A. Paschos, Phys. Rev. D **71**, 074003 (2005).
[18] T. Leitner, L. Alvarez-Ruso, and U. Mosel, Phys. Rev. C **73**, 065502 (2006).
[19] O. Lalakulich, E. A. Paschos, and G. Piranishvili, Phys. Rev. D **74**, 014009 (2006).
[20] G. M. Radecky *et al.*, Phys. Rev. D **25**, 1161 (1982).
[21] T. Kitagaki *et al.*, Phys. Rev. D **34**, 2554 (1986).
[22] S. Galster *et al.*, Nucl. Phys. **B32**, 221 (1971).
[23] T. Ericson and W. Weise, *Pions and Nuclei* (Clarendon Press, Oxford, 1988).
[24] Th. Wilbois, P. Wilhelm, and H. Arenhovel, Phys. Rev. C **57**, 295 (1998); A. J. Buchmann, E. Hernández, and A. Faessler, Phys. Rev. C **55**, 448 (1997); O. Hanstein, D. Drechsel, and L. Tiator, Phys. Lett. B **385**, 45 (1996); M. Benmerrouche and N. C. Mukhopadhyay, Phys. Rev. D **46**, 101 (1992), and references therein.
[25] K. Joo *et al.* (CLAS Collaboration), Phys. Rev. Lett. **88**, 122001 (2002).
[26] J. Campbell *et al.*, Phys. Rev. Lett. **30**, 335 (1973).
[27] S. J. Barish *et al.*, Phys. Rev. D **19**, 2521 (1979).
[28] T. Kitagaki *et al.*, Phys. Rev. D **42**, 1331 (1990).
[29] P. Salin, Nuovo Cimento A **48**, 506 (1967); J. Bijtebier, Nucl. Phys. **B21**, 158 (1970).
[30] C. Alexandrou, Th. Leontiou, J. W. Negele, and A. Tsapalis, Phys. Rev. Lett. **98**, 052003 (2007).
[31] A. Gil, J. Nieves, and E. Oset, Nucl. Phys. **A627**, 543 (1997).
[32] E. Hernández, J. Nieves, and M. Valverde, Phys. Lett. B **647**, 452 (2007).
[33] W. M. Alberico, S. M. Bilenky, C. Giunti, and C. Maieron, Z. Phys. C **70**, 463 (1996).
[34] G. T. Garvey, W. C. Louis, and D. H. White, Phys. Rev. C **48**, 761 (1993).
[35] A. Gómez-Nicola, J. Nieves, J. R. Pelaez, and E. Ruiz-Arriola, Phys. Lett. B **486**, 77 (2000); Phys. Rev. D **69**, 076007 (2004).
[36] J. Nieves, M. Pavon-Valderrama, and E. Ruiz-Arriola, Phys. Rev. D **65**, 036002 (2002).
[37] S. J. Barish *et al.*, Phys. Rev. D **16**, 3103 (1977).
[38] N. J. Baker *et al.*, Phys. Rev. D **23**, 2499 (1981).
[39] T. Bolognese, J. P. Engel, J. L. Guyonnet, and J. L. Riester *et al.*, Phys. Lett. B **81**, 393 (1979).
[40] J. Bell *et al.*, Phys. Rev. Lett. **41**, 1012 (1978).
[41] P. Allen *et al.*, Nucl. Phys. **B264**, 221 (1986).
[42] J. Liu, N. C. Mukhopadhyay, and L. Zhang, Phys. Rev. C **52**, 1630 (1995).
[43] K. M. Watson, Phys. Rev. **95**, 228 (1954).
[44] M. Sajjad Athar, S. Ahmad, and S. K. Singh, Phys. Rev. D **75**, 093003 (2007).
[45] G. Karpman, R. Leonardi, and F. Strocchi, Phys. Rev. **174**, 1957 (1968).
[46] F. Cannata, R. Leonardi, and F. Strocchi, Phys. Rev. D **1**, 191 (1970).
[47] W. Krenz *et al.*, Nucl. Phys. **B135**, 45 (1978).
[48] M. Derrick *et al.*, Phys. Lett. B **92**, 363 (1980); **95**, 461(E) (1980).
[49] M. Derrick *et al.*, Phys. Rev. D **23**, 569 (1981).
[50] E. A. Hawker, in *Proceedings of the Second International Workshop on Neutrino-Nucleus Interactions in the Few GeV Region, Irvine, California, 2002*, http://www.ps.uci.edu/~nuint/proceedings/hawker.pdf.
[51] E. Hernández, J. Nieves, S. K. Singh, M. Valverde, and M. J. Vicente-Vacas (unpublished).